© 2015. Published by The Company of Biologists Ltd | Development (2015) 142, 1113-1124 doi:10.1242/dev.117424

RESEARCH ARTICLE

Evolutionarily conserved regulation of hypocretin neuron specification by Lhx9

Justin Liu[1], Florian T. Merkle[2,3], Avni V. Gandhi[1], James A. Gagnon[2], Ian G. Woods[2,*], Cindy N. Chiu[1], Tomomi Shimogori[4], Alexander F. Schier[2,3,5] and David A. Prober[1,‡]

ABSTRACT

Loss of neurons that express the neuropeptide hypocretin (Hcrt) has been implicated in narcolepsy, a debilitating disorder characterized by excessive daytime sleepiness and cataplexy. Cell replacement therapy, using Hcrt-expressing neurons generated *in vitro*, is a potentially useful therapeutic approach, but factors sufficient to specify Hcrt neurons are unknown. Using zebrafish as a high-throughput system to screen for factors that can specify Hcrt neurons *in vivo*, we identified the LIM homeobox transcription factor Lhx9 as necessary and sufficient to specify Hcrt neurons. We found that Lhx9 can directly induce *hcrt* expression and we identified two potential Lhx9 binding sites in the zebrafish *hcrt* promoter. Akin to its function in zebrafish, we found that Lhx9 is sufficient to specify *Hcrt*-expressing neurons in the developing mouse hypothalamus. Our results elucidate an evolutionarily conserved role for Lhx9 in Hcrt neuron specification that improves our understanding of Hcrt neuron development.

KEY WORDS: Hypocretin, Lhx9, Zebrafish

INTRODUCTION

The neuropeptide hypocretin (Hcrt) is conserved among vertebrates and plays key roles in regulating sleep, metabolism, feeding, anxiety, reward and addiction (Bonnavion and de Lecea, 2010; Tsujino and Sakurai, 2009). Hcrt is particularly important in promoting arousal, as loss of Hcrt neurons is thought to cause narcolepsy (Peyron et al., 2000; Thannickal et al., 2000), a disorder characterized by daytime sleepiness, fragmented sleep-wake states and cataplexy. Narcolepsy affects approximately 1 in 2000 individuals, but treatments are limited to symptom management (Dauvilliers et al., 2007). Despite the importance of the Hcrt system, little is known about the developmental processes that give rise to Hcrt neurons. A recent study found that mice lacking the LIM domain homeobox transcription factor Lhx9 had fewer Hcrt neurons (Dalal et al., 2013), suggesting that Lhx9 is required to specify a subset of Hcrt neurons. However, overexpression of *Lhx9* in adult mice or in a mouse neuroblastoma cell line had no effect on Hcrt cell number or expression. Therefore, the role of Lhx9 in Hcrt neuron specification remains unclear and the set of factors sufficient to specify Hcrt neurons remains unknown. Identifying these factors would help elucidate how a key neural circuit that governs sleep is established, and could lead to novel therapies for narcolepsy.

The zebrafish *Danio rerio* is a powerful genetic model of vertebrate development that provides several advantages for studying Hcrt neuron specification. First, the hypothalamus is remarkably conserved (Blackshaw et al., 2010; Machluf et al., 2011; Tessmar-Raible et al., 2007), suggesting that developmental mechanisms identified in zebrafish are likely to be relevant to mammals. Several studies have shown that the mammalian Hcrt system is functionally and anatomically conserved in zebrafish (Chiu and Prober, 2013; Elbaz et al., 2013). Whereas the rodent hypothalamus contains thousands of Hcrt neurons, larval and adult zebrafish contain only approximately 10 and 40 Hcrt neurons, respectively (Faraco et al., 2006; Kaslin et al., 2004), making zebrafish a more tractable system to study Hcrt neuron development. Second, the external development and transparency of zebrafish embryos facilitate the observation of developing Hcrt neurons. Third, high-throughput genetic gain- and loss-of-function assays facilitate efficient screens to identify developmental regulators. We exploited these features of zebrafish to identify genes that regulate Hcrt neuron specification.

RESULTS

Microarray analysis identifies transcripts enriched in Hcrt neurons

Previous studies showed that the number of Hcrt neurons in zebrafish and rodents increases as animals develop and mature to adulthood (Faraco et al., 2006; Kaslin et al., 2004; Sawai et al., 2010). We reasoned that cell-autonomous factors required to specify Hcrt neurons might still be expressed in Hcrt neurons shortly after they are specified. To identify these factors, we generated transgenic zebrafish that express monomeric red fluorescent protein (mRFP) in Hcrt neurons and enhanced green fluorescent protein (EGFP) in neurons that express the hypothalamic neuropeptide QRFP (supplementary material Fig. S1). QRFP has been implicated in regulating locomotor activity (Takayasu et al., 2006), feeding (Chartrel et al., 2003; Takayasu et al., 2006) and nociception (Yamamoto et al., 2009) in rodents, and sleep/wake behaviors in zebrafish (C.N.C., A. Chen and D.A.P., unpublished).

Expression of *hcrt* and *qrfp* (*si:ch211-185o22.2*, incorrectly annotated as lincRNA) is first detected in zebrafish embryos at 24 h post-fertilization (hpf) in bilateral hypothalamic nuclei of 4-6 cells (Fig. 1A,B), which expand to 10-15 cells by 120 hpf (Fig. 1C,D). Hcrt and QRFP are expressed in neighboring neurons throughout development, but are never co-expressed within the same cells (Fig. 1B,D). To identify genes with enriched expression in Hcrt neurons, we dissociated pools of 100-300 *Tg(hcrt:mRFP, qrfp:EGFP)* embryos at 26 hpf into single cells and isolated EGFP- and mRFP-expressing neurons by fluorescence-activated cell sorting (FACS) (Fig. 1E; supplementary material Fig. S2). FACS gates for

[1]Division of Biology and Biological Engineering, California Institute of Technology, Pasadena, CA 91125, USA. [2]Departments of Molecular and Cellular Biology, and Stem Cell and Regenerative Biology, Harvard University, Cambridge, MA 02138, USA. [3]Harvard Stem Cell Institute, Harvard University, Cambridge, MA 02138, USA. [4]Brain Science Institute, RIKEN, Saitama 351-0198, Japan. [5]Division of Sleep Medicine, Harvard University, Cambridge, MA 02115, USA.
*Present address: Department of Biology, Ithaca College, Ithaca, NY 14850, USA.

‡Author for correspondence (dprober@caltech.edu)

Received 3 September 2014; Accepted 15 January 2015

Development (2015) 142, 1113-1124 doi:10.1242/dev.117424

EGFP and mRFP populations were set using wild-type embryos (0/10,000 $EGFP^+$ or $mRFP^+$ events). In a representative experiment, we obtained 250 $EGFP^+$ cells and 528 $mRFP^+$ cells from 150 *Tg(hcrt:mRFP, qrfp:EGFP)* double-heterozygous embryos. To verify the fidelity of FACS, we visually screened for fluorescence in sorted cells (Fig. 1F). In the sorted *qrfp:EGFP* population, we observed EGFP in 99/117 cells (85%) but no mRFP (0/117). In the sorted *hcrt:mRFP* population, we observed mRFP in 110/146 cells (75%) but no EGFP (0/146). These values are likely to underestimate the purity of the sorted cells because FACS is more sensitive than visual inspection.

We extracted total mRNA from each cellular fraction and used cDNA microarrays to compare gene expression in Hcrt and QRFP neurons. We also compared gene expression in Hcrt neurons with expression in neurons labeled by a pan-neuronal marker, *Tg(elavl3:EGFP)*, and with expression in subtypes of sensory neurons: *Tg(trpa1b:EGFP)*, *Tg(isl1:Gal4VP16, 14xUAS:EGFP)* and *Tg(p2rx3b:EGFP)*. *elavl3* encodes an RNA-binding protein that is expressed in most postmitotic neurons (Park et al., 2000); *trpa1b* encodes a transient receptor potential (TRP) channel that is activated by chemical irritants (Prober et al., 2008); *p2rx3b* encodes an ATP-gated ion channel in non-peptidergic nociceptors (Kucenas et al., 2006); and *islet1* (*isl1*) encodes a LIM homeobox transcription factor that is expressed in sensory neurons and motoneurons (Higashijima et al., 2000). We used an *isl1* enhancer that drives expression in a subset of sensory neurons (Sagasti et al., 2005). The *Tg(trpa1b:EGFP)* and *Tg(isl1:Gal4VP16, 14xUAS:EGFP)* lines express EGFP in largely non-overlapping subsets of trigeminal and Rohon-Beard sensory neurons (Pan et al., 2012). *p2rx3b* is expressed in all cells labeled in *Tg(trpa1b:EGFP)* embryos and in a quarter of cells labeled in *Tg(isl1:Gal4VP16, 14xUAS:EGFP)* embryos.

These samples allowed five pairwise comparisons of Hcrt neurons with different purified neuron populations (supplementary material Fig. S2 and Table S1). This analysis provided greater statistical power than previous studies that compared Hcrt neurons with a single outgroup (Cvetkovic-Lopes et al., 2010; Dalal et al., 2013). An additional study examined changes in gene expression across multiple brain regions after the onset of narcolepsy (Honda et al., 2009); however, this approach is unlikely to identify developmentally relevant transcripts. We focused on 19 highly ranked genes that encode transcription factors or secreted proteins (Tables 1 and 2), as both classes of proteins have well-established roles in neural development (Blackshaw et al., 2010; Wilson and Houart, 2004); as expected, *hcrt* was the most highly enriched gene in Hcrt neurons (Table 2). The complete microarray dataset is available through ArrayExpress, accession number E-MTAB-3317.

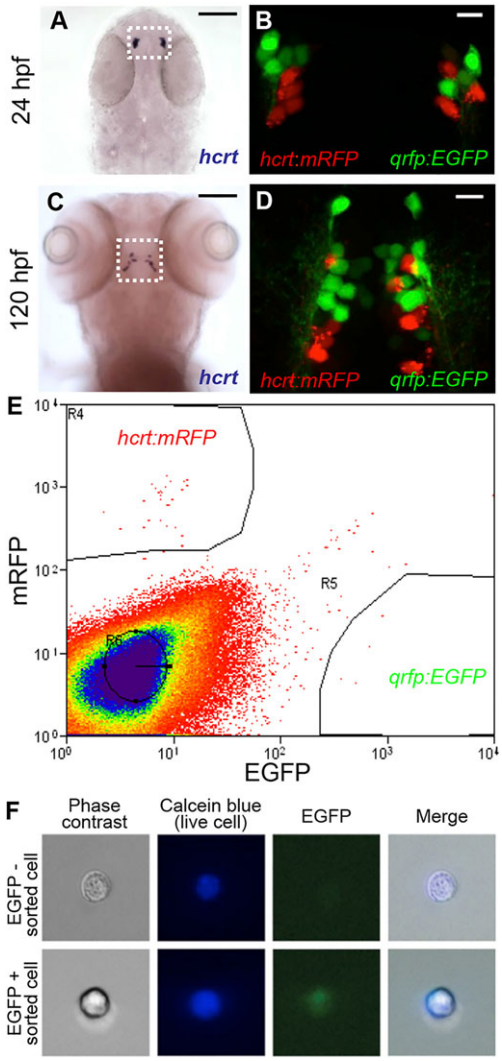

Fig. 1. Isolation of *hcrt*- and *qrfp*-expressing neurons from zebrafish embryos. (A-D) *hcrt* is expressed in bilateral populations of 4-6 neurons at 24 hpf (A) and 10-15 neurons at 120 hpf (C). Fluorescence in *Tg(hcrt:mRFP, qrfp:EGFP)* embryos is first observed at ~24 hpf. mRFP- and EGFP-labeled neurons are intermingled, but the markers are never co-expressed in the same cell (B,D). Boxed regions in A,C are shown at higher magnification in B,D. Scale bars: 100 µm in A,C; 10 µm in B,D. (E) *Tg(hcrt:mRFP, qrfp:EGFP)* embryos were dissociated into single cells at 26 hpf and mRFP- and EGFP-expressing cells were isolated by FACS. The proportion of mRFP-positive and EGFP-positive cells was consistent with the number of Hcrt and QRFP neurons, respectively, in a 26 hpf embryo. (F) EGFP is observed in a sorted *qrfp:EGFP*$^+$ cell.

Expression patterns of candidate genes validate the microarray results

High quality *in situ* hybridization (ISH) images were available in the ZFIN database for seven candidate genes (supplementary material Fig. S3). We determined the expression patterns of the remaining 12 genes using ISH on 24 hpf embryos (Fig. 2; supplementary material Fig. S3 and Movie 1). We found that 11 of 14 genes encoding transcription factors and five of five genes encoding secreted proteins are expressed in a similar or overlapping domain to Hcrt neurons. Some genes, such as the transcription factor *lhx9*, are expressed in all Hcrt cells throughout early development (supplementary material Fig. S4). The microarray therefore accurately reported the expression of most candidate genes.

Lhx9 is sufficient to specify Hcrt neurons

To determine whether any candidate gene is sufficient to induce specification of Hcrt neurons, we cloned each gene downstream of a heat shock-inducible promoter in a vector containing Tol2 transposase sites, and injected the plasmid together with *tol2* transposase mRNA into zebrafish embryos at the 1-cell stage. As a result, the plasmid inserts into the genome of a random subset of cells. We transiently overexpressed each gene by performing a heat shock at 24 hpf (Fig. 3A). This approach provides an efficient, inducible method for overexpressing different candidate genes in 10-20% of cells (Fig. 3C).

Quantification of hypothalamic Hcrt neurons using ISH at 120 hpf showed no significant differences between larvae overexpressing candidate genes and controls (supplementary material Fig. S5). However, 14% of larvae overexpressing *lhx9* contained additional, ectopic Hcrt expression in the medial hindbrain (7/50 larvae; Fig. 3E,F). These larvae had 2.7 ectopic

Development (2015) 142, 1113-1124 doi:10.1242/dev.117424

Table 1. Transcription factors enriched in Hcrt neurons

Gene	GenBank accession number	Fold increase*	ZFIN *in situ* available	Expression pattern at 24 hpf	Possible expression in Hcrt neurons
hmx2	NM_001115098	120	No	Hypothalamus‡, spinal cord, lateral line	Yes
hmx3	NM_131634	106	Yes	Hypothalamus, telencephalon, hindbrain, spinal cord, ear, lateral line	Yes
npas4	NM_001045321	106	No	Brain ubiquitous	Yes
lhx9	AB188254	99	No	Hypothalamus, telencephalon, hindbrain, spinal cord	Yes
sox1a	NM_001002483	70	Yes	Hypothalamus, telencephalon, hindbrain, lens, lateral line	Yes
nr4a2	NM_001002406	36	Yes	Telencephalon, hindbrain	No
mybbp1a	NM_001002042	25	Yes	Hypothalamus, telencephalon, hindbrain, retina, myotomes	Yes
rfx2	NM_001013278	22	Yes	Hypothalamus, telencephalon, spinal cord, pronephric ducts	Yes
tshz2	NM_173485	21	No	Hypothalamus, telencephalon, spinal cord, lateral line	Yes
bhlhe40	NM_212679	17	Yes	Retina, epiphysis, myotomes, neural crest	No
tead1	NM_212847	15	No	Hypothalamus, telencephalon, hindbrain	Yes
cited2	NM_001044982	14	No	Hypothalamus, telencephalon, hindbrain	Yes
ets2	NM_001023580	12	Yes	Hypothalamus, telencephalon, endothelium	Yes
cbx4	BC171352	10	No	Ventral hypothalamus, telencephalon, hindbrain	No

*Fold increase indicates the expression level of a gene in Hcrt neurons relative to its expression in the other neuronal subtypes analyzed by microarray.
‡Genes expressed in the hypothalamus may be expressed in a broad or restricted pattern.

Hcrt cells on average, a 17% increase in the total number of Hcrt neurons. No other candidate gene was sufficient to specify ectopic Hcrt neurons. Like endogenous hypothalamic Hcrt neurons, the ectopic Hcrt neurons expressed *vesicular glutamate transporter 1* (*vglut1*; *slc17a7a*) and *prodynorphin* (*pdyn*) (Fig. 4). *vglut1* is widely expressed in the hypothalamus and hindbrain, but its expression is particularly strong in Hcrt neurons (Fig. 4A,B; supplementary material Movie 2). Hcrt neurons also exhibit intense, punctate *pdyn* labeling (Fig. 4D,E; supplementary material Movie 3) that is likely to indicate sites of transcription (Hanisch et al., 2012; Kosman et al., 2004). We did not detect significant expression of *vglut2a* (*slc17a6b*) or *vglut2b* (*slc17a6a*) in Hcrt neurons (supplementary material Figs S8 and S9).

lhx9 overexpression generated more cells in the medial hindbrain with strong *vglut1* expression or punctate *pdyn* expression than ectopic Hcrt cells (Fig. 4C,F), suggesting that Lhx9 can specify multiple cell types. Indeed, most *lhx9*-overexpressing neurons also expressed *qrfp* at 1 h post-heat shock (data not shown), and we observed an average of three ectopic QRFP neurons in the medial hindbrain 96 h after Lhx9 overexpression (8/40 larvae; supplementary material Fig. S6; note that *lhx9* was enriched in *hcrt* neurons compared with *elavl3*, *isl1*, *trpa1b* and *p2rx3b* neurons, but not compared with *qrfp* neurons, in the microarray analysis). Similar to Hcrt neurons, both hypothalamic and ectopic QRFP neurons express Lhx9 (supplementary material Figs S6 and S7). Ectopic QRFP neurons did not co-express *hcrt* (0/24 QRFP neurons), suggesting that they remain developmentally distinct populations.

Both mammalian and zebrafish Hcrt neurons project to several brain regions, including the noradrenergic locus coeruleus (LC) (Horvath et al., 1999; Prober et al., 2006). To determine whether ectopic Hcrt neurons project to this endogenous Hcrt neuron target, we overexpressed *lhx9* in transgenic zebrafish that expressed the photoconvertible fluorescent protein Kaede in Hcrt neurons and EGFP in *dopamine beta-hydroxylase* (*dbh*)-expressing LC neurons (supplementary material Fig. S1). We used a 405 nm laser to photoconvert Hcrt neurons in the hindbrain, but not in the hypothalamus, from green to red fluorescence. We observed that all red fluorescent ectopic Hcrt neurons project to the LC (15/15 neurons) (Fig. 5A,C). By contrast, stochastic labeling of neurons in the medial hindbrain with an *elavl3:Kaede* transgene indicates that only ~20% of cells in this region target the LC (9/50 neurons) (Fig. 5B,C). These experiments indicate that Lhx9 is sufficient to

Table 2. Secreted proteins enriched in Hcrt neurons

Gene	GenBank accession number	Fold increase*	ZFIN *in situ* available	Expression pattern at 24 hpf	Possible expression in Hcrt neurons
hcrt	NM_001077392	248	No	Hypothalamus	–
cart4	NM_001082932	130	No	Hypothalamus, ventral hindbrain	Yes
igsf21	NM_001034184	85	Yes	Hypothalamus, ventral hindbrain	Yes
trh	NM_001012365	45	No	Hypothalamus, ventral hindbrain	Yes
endouc	NM_001044974	43	No	Hypothalamus, telencephalon, lens, posterior midbrain, hindbrain, lateral line	Yes
glipr1b	NM_200575	19	No	Hypothalamus, telencephalon, hindbrain	Yes

*Fold increase indicates the expression level of a gene in Hcrt neurons relative to its expression in the other neuronal subtypes analyzed by microarray.

Development (2015) 142, 1113-1124 doi:10.1242/dev.117424

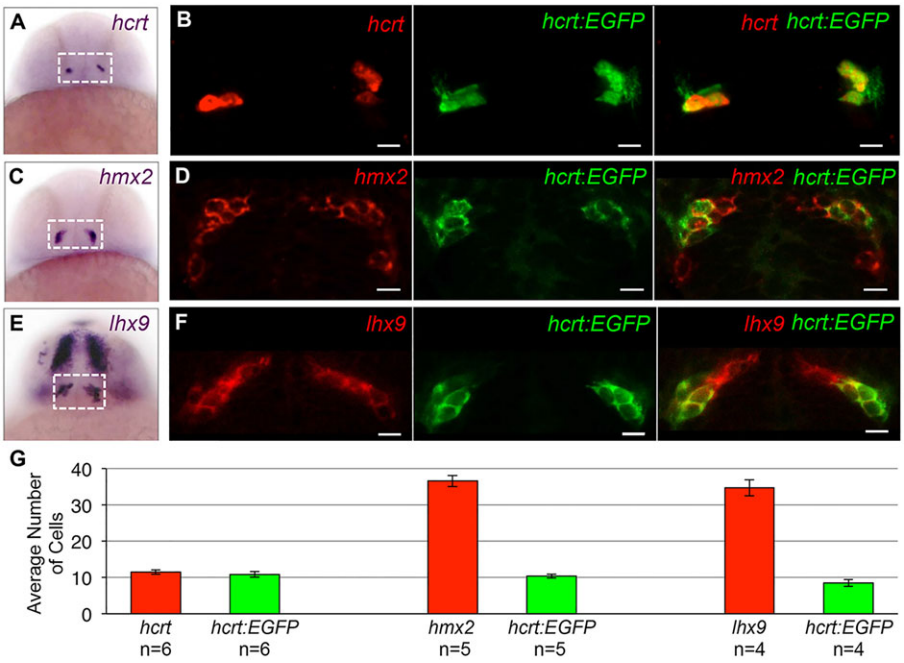

Fig. 2. Examples of expression patterns of Hcrt neuron-enriched genes. (A,C,E) ISH performed on 24 hpf zebrafish embryos using probes specific for *hcrt*, *hmx2* and *lhx9*. Dashed boxes indicate the hypothalamic regions shown in B,D,F. (B,D,F) A 1.25-µm confocal section of fluorescent ISH (red) and *hcrt:EGFP* immunofluorescence (green). All *hcrt:EGFP* neurons express *hmx2* and *lhx9*. *hmx2* expression extends ventrally (C,D) and *lhx9* is expressed in broader domains of the telencephalon and diencephalon (E,F), as well as the hindbrain and spinal cord (not shown). Supplementary material Movie 1 contains the complete confocal image stack for F. (G) Mean±s.e.m. number of cells in the boxed regions in A,C,E. *n*, number of brains. Scale bars: 10 µm.

specify Hcrt neurons *in vivo* that are genetically and anatomically similar to endogenous Hcrt neurons.

Lhx9 is necessary for Hcrt neuron specification

To test whether Lhx9 is necessary for Hcrt neuron specification, we used a splice-blocking morpholino to knock down *lhx9* expression. RT-PCR revealed robust inhibition of *lhx9* mRNA splicing, and thus of functional Lhx9 protein production, up to 72 hpf (supplementary material Fig. S10). Morphants had ∼40% fewer Hcrt neurons when assessed by ISH (Fig. 6C), and the remaining Hcrt neurons had reduced *hcrt* expression compared with embryos injected with a 5 bp mismatch control morpholino (Fig. 6A,B). qRT-PCR revealed that *lhx9* morphants express 62% less *hcrt* transcript than control morphants (s.e.m.=5%, *n*=3 replicates), confirming that Hcrt neurons that persist in *lhx9* morphants contain less *hcrt* transcript than controls.

To determine whether the missing Hcrt neurons in *lhx9* morphants lack *hcrt* expression or were absent, we examined the effect of *lhx9* knockdown on *vglut1* and *pdyn* (supplementary material Fig. S11). *lhx9* morphants had no gross defects in *vglut1* expression compared with controls. However, the number of cells with intense punctate *pdyn* expression, which includes all Hcrt cells, was reduced by ∼40%. The loss of Hcrt cells was not caused by nonspecific morpholino-induced apoptosis, as embryos co-injected with an apoptosis-suppressing *p53* (*tp53*) morpholino (Robu et al., 2007) and the *lhx9* morpholino showed the same phenotype (Fig. 6C). Furthermore, *lhx9* morpholino-injected embryos stained with Acridine Orange, which labels apoptotic cells, showed no increase in apoptosis (supplementary material Fig. S12A-E). The morpholino phenotype was partially rescued by co-injecting the *lhx9* morpholino with the *hs:lhx9* plasmid and performing a heat shock at 24 hpf (supplementary material Fig. S12F,G), indicating that the reduction in Hcrt cells was a specific effect of *lhx9* knockdown. *hcrt* expression was weaker in rescued cells than in endogenous Hcrt neurons, presumably because rescued cells only received a pulse of *lhx9*

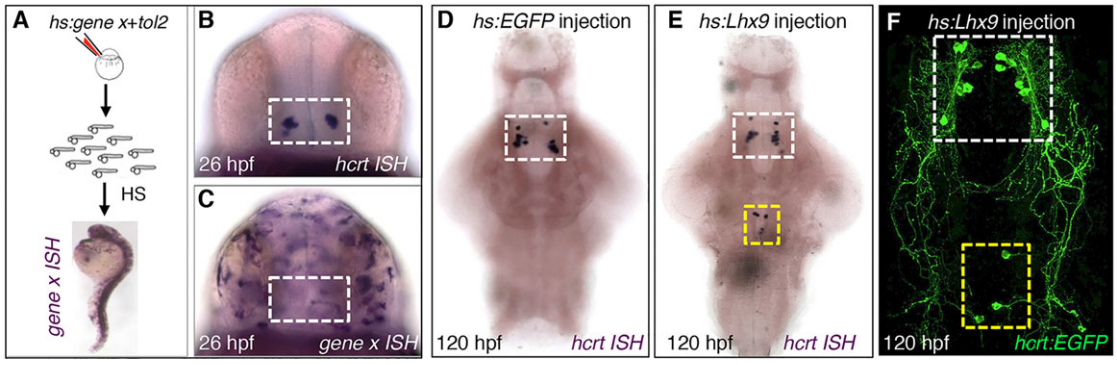

Fig. 3. Transient *lhx9* overexpression induces ectopic Hcrt neurons. (A) Zebrafish embryos were injected with *tol2* transposase mRNA and a plasmid in which a heat shock-inducible promoter regulates the expression of a candidate gene (*hs:gene x*). (B,C) Anterior views of 26 hpf embryos after ISH showing endogenous *hcrt* expression (B) and mosaic expression of *gene x* 1 h after heat shock (C). Approximately 10-20% of cells overexpress *gene x*. White box in B,C indicates the hypothalamus. (D) Control embryos injected with an *hs:EGFP* plasmid exhibit normal *hcrt* expression at 120 hpf. (E) Embryos overexpressing *lhx9* contain ectopic Hcrt cells that are dorsal and caudal relative to endogenous Hcrt neurons. (F) Ectopic Hcrt cells exhibit neuronal morphology, as visualized using *Tg(hcrt:EGFP)* larvae. White and yellow boxes in D-F indicate endogenous and ectopic Hcrt cells, respectively.

Development (2015) 142, 1113-1124 doi:10.1242/dev.117424

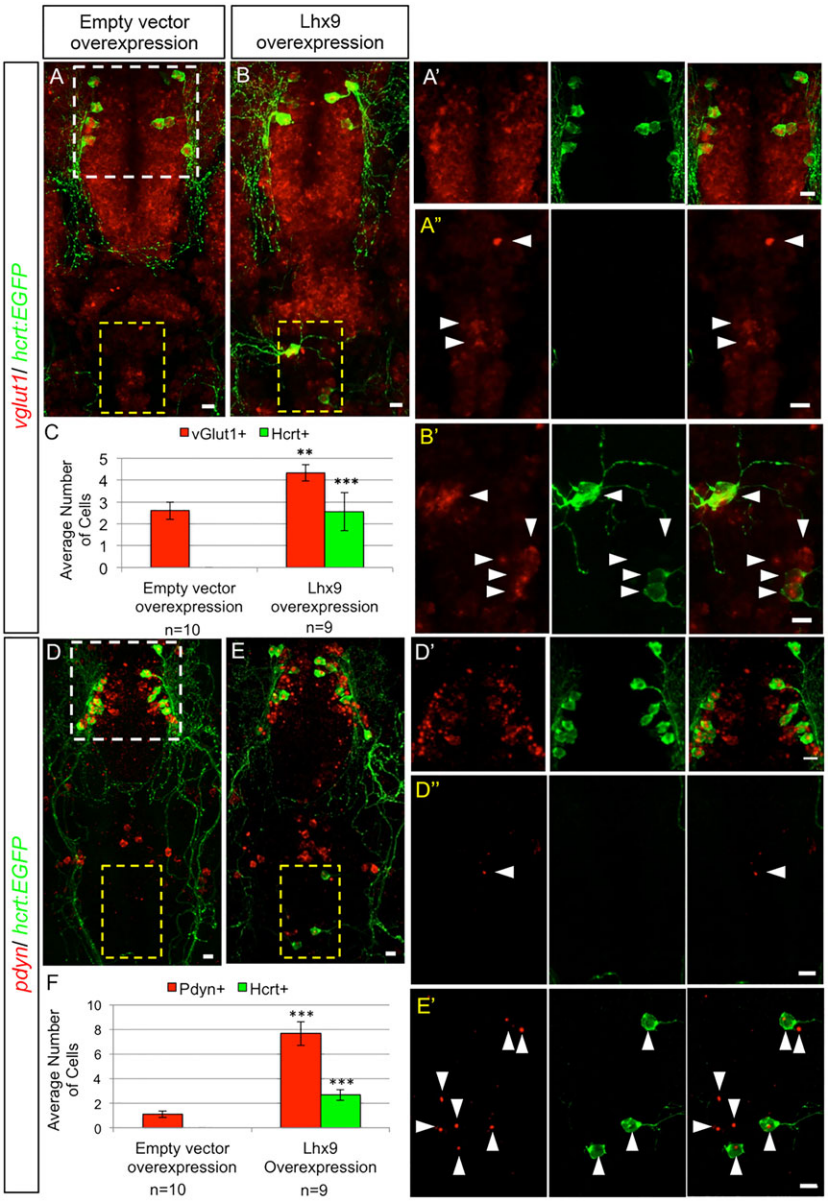

Fig. 4. Hypothalamic and ectopic Hcrt neurons share biomarkers. Confocal projections of 120 hpf *Tg(hcrt:EGFP)* zebrafish larval brains containing endogenous and ectopic Hcrt neurons labeled with an anti-EGFP antibody and fluorescent ISH probes specific for *vglut1* (A,B) and *pdyn* (D,E). White and yellow boxes in A,D indicate endogenous Hcrt neurons in the hypothalamus and endogenous *vglut1* and *pdyn* expression in the hindbrain, respectively, shown enlarged in A′,D′ and in A″,D″. Yellow boxes in B,E indicate ectopic Hcrt neurons, as enlarged in B′,E′. All hypothalamic and ectopic Hcrt neurons express *vglut1* and *pdyn*. Larvae injected with *hs:lhx9* and heat-shocked at 24 hpf contain ectopic Hcrt neurons in the hindbrain and more cells with strong *vglut1* (B,B′) and punctate *pdyn* (E,E′) expression, compared with controls injected with an empty heat shock vector (A,A″,D,D″). Arrowheads indicate cells with strong *vglut1* or *pdyn* expression. (C,F) Mean±s.e.m. number of cells in the yellow boxed regions. *n*, number of brains quantified. ***P*<0.01, ****P*<0.001 compared with empty heat shock vector (Student's *t*-test). Scale bars: 10 µm.

whereas endogenous Hcrt neurons continuously express *lhx9* (supplementary material Fig. S4). We also tested morpholinos against *hmx2* or *hmx3*, which were more highly enriched in Hcrt neurons than *lhx9* in our microarray analysis. Although RT-PCR confirmed that these morpholinos were effective, they had no effect on Hcrt neuron specification (data not shown).

Some Hcrt neurons persisted in *lhx9* morphants, possibly owing to incomplete *lhx9* knockdown (supplementary material Fig. S10) or because Lhx9 is only necessary to specify a subset of Hcrt neurons, as in mice (Dalal et al., 2013). To distinguish between these possibilities, we used the CRISPR/Cas9 system (Jao et al., 2013; Hwang et al., 2013) to introduce mutations into *lhx9*. We co-injected Cas9 protein (Gagnon et al., 2014) with a set of short guide RNAs (sgRNAs) that target *lhx9* into embryos at the 1-cell stage to generate biallelic mutations and a loss-of-function phenotype in the injected animals (Jao et al., 2013). Embryos injected with Cas9+*lhx9* sgRNAs had 90% fewer Hcrt cells than embryos injected with Cas9 alone (Fig. 6D-F). Furthermore, over half of brain hemispheres of embryos injected with Cas9+*lhx9* sgRNAs completely lacked Hcrt cells, whereas embryos injected with Cas9 alone had at least three Hcrt cells in each brain hemisphere (Fig. 6G). This phenotype is unlikely to be due to off-target effects of particular sgRNAs, as we observed a similar, albeit weaker, phenotype in embryos injected with Cas9 and independent subsets of *lhx9* sgRNAs (supplementary material Fig. S13). We conclude that *lhx9* is necessary to specify all Hcrt neurons in zebrafish embryos.

Because *lhx9* overexpression was sufficient to specify QRFP neurons, we asked whether *lhx9* is also necessary for QRFP neuron specification. We observed 63% fewer QRFP neurons in embryos injected with Cas9+*lhx9* sgRNAs compared with Cas9 alone, and over 20% of brain hemispheres lacked QRFP neurons (supplementary material Fig. S13). Injection of embryos with Cas9 and subsets of *lhx9* sgRNAs produced a similar, albeit weaker, phenotype. We conclude that *lhx9* is necessary to specify all QRFP neurons.

Lhx9 directly promotes *hcrt* expression

As Lhx9 is a transcription factor, we hypothesized that it might promote *hcrt* expression directly. A previous study tested this

Development (2015) 142, 1113-1124 doi:10.1242/dev.117424

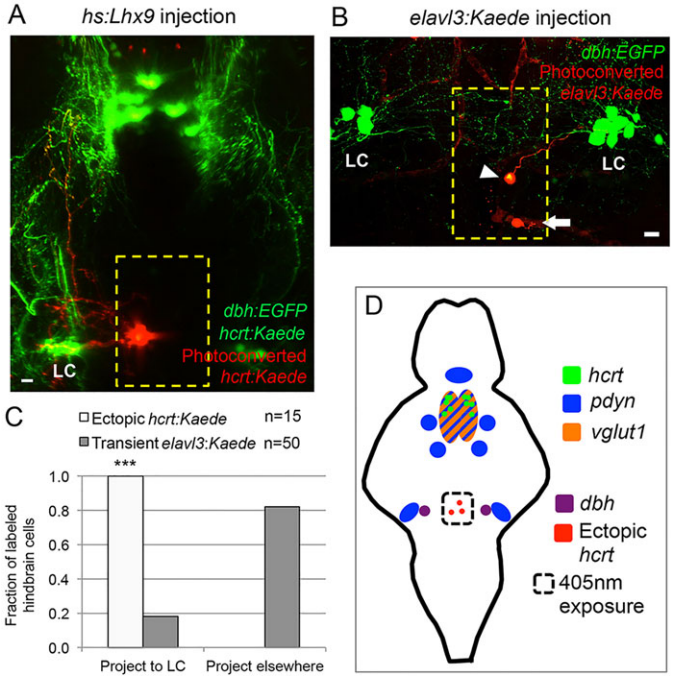

Fig. 5. Ectopic Hcrt neurons project to the locus coeruleus. (A) Confocal projection of a 120 hpf *Tg(hcrt:Kaede, dbh:EGFP)* larva injected with an *hs:lhx9* plasmid shows that ectopic photoconverted Hcrt cells in the medial hindbrain (red) project to the locus coeruleus (LC). (B) Confocal projection of a 120 hpf *Tg (dbh:EGFP)* larva injected with an *elavl3:Kaede* plasmid to stochastically label neurons shows that some neurons in the medial hindbrain project to the LC (arrowhead) whereas others do not (arrow; axon projects orthogonally to the image). (C) All ectopic Hcrt neurons project to the LC, but only 20% of *elavl3:Kaede*-labeled cells in the same brain region project to the LC. *n*, number of neurons analyzed. ***P<0.001 compared with *elavl3:Kaede* (Fisher's exact test). Yellow boxes in A,B indicate the regions used for quantification. (D) Schematic of *hcrt*, *pdyn* and *vglut1* expression in the ventral zebrafish brain at 120 hpf. The locations of ectopic Hcrt neurons, *dbh*-expressing LC neurons and the photoconverted region are shown. Scale bars: 10 µm.

hypothesis *in vitro* by co-expressing *Lhx9* and a mouse *Hcrt* promoter-luciferase reporter in a neuroblastoma cell line, and *in vivo* by lentiviral transduction of *Lhx9* into the hypothalamus of adult mice, but observed no effect on *Hcrt* expression (Dalal et al., 2013). However, when we performed double-fluorescent ISH against *lhx9* and *hcrt* on zebrafish embryos fixed 1 h after heat shock, we observed *hcrt* expression in almost all *lhx9*-overexpressing cells (Fig. 7A; supplementary material Fig. S14 and Movie 4). The number of ectopic *lhx9*- and *hcrt*-expressing cells is reduced at 8 h after heat shock (supplementary material Fig. S14D), and few ectopic cells are observed 24 h after heat shock (supplementary material Fig. S14F), similar to the number observed at 120 hpf (supplementary material Fig. S14H). Importantly, ectopic *hcrt*-expressing neurons also express ectopic *lhx9* at all time points. These findings support the hypothesis that Lhx9 can directly regulate *hcrt* expression.

A previous study identified an Lhx9 binding site upstream of the *wilms tumor 1* gene (Wilhelm and Englert, 2002), and we observed two similar sites in the zebrafish *hcrt* promoter (sites A and B) (Fig. 7B,C). Notably, site A corresponds to a region previously shown to be important for *hcrt* expression in zebrafish (Faraco et al., 2006). We tested whether these sites are necessary for endogenous (i.e. hypothalamic) and Lhx9-induced ectopic *hcrt* expression by injecting wild-type embryos with plasmids containing the *hcrt* promoter, in which one or both putative Lhx9 binding sites were mutated, placed upstream of EGFP. Each plasmid also contained a heat shock-inducible *lhx9* transgene downstream of the EGFP reporter. Thus, any cell that contains the plasmid will have both the *hcrt:*EGFP reporter and the *hs:lhx9* transgene. Injected embryos were heat-shocked at 24 hpf and analyzed at 120 hpf for hypothalamic and ectopic *hcrt:*EGFP-expressing neurons (Fig. 7D, HS samples). Some injected embryos were not heat-shocked (Fig. 7D, no HS samples) to determine whether the putative Lhx9 binding sites are required for EGFP expression in the endogenous Hcrt domain alone. Mutating site A, either by deletion or by scrambling every third nucleotide, reduced the number and intensity of endogenous and ectopic cells labeled with EGFP as compared with the wild-type *hcrt* promoter (Fig. 7C,D,F-H). Scrambling the sequences of both sites A and B virtually abolished EGFP expression (Fig. 7D,I). Notably, ectopic *hcrt* cells were never observed for the double-mutant reporter. These experiments indicate that sites A and B are crucial for *hcrt* expression *in vivo*.

To test whether Lhx9 can interact with these sites, we performed an EMSA using the zebrafish Lhx9 homeodomain (Lhx9 HD) and radiolabeled oligonucleotides that include the wild-type or scrambled sequences for sites A and B. We found that Lhx9 HD binds to the wild-type site A probe, but not to the scrambled site A probe (Fig. 7J). We failed to observe an interaction between Lhx9 HD and the site B probe (data not shown), possibly owing to non-optimal *in vitro* binding or electrophoresis conditions. This result indicates that Lhx9 can bind to site A *in vitro* and suggests that Lhx9 directly regulates *hcrt* expression *in vivo* via binding to this site.

Lhx9 overexpression in mouse embryos induces Hcrt neuron specification

A previous study that overexpressed *Lhx9* in the hypothalamus of adult mice observed no effect on Hcrt neuron specification (Dalal et al., 2013). To determine whether Lhx9 can promote Hcrt neuron specification earlier in mammalian development, we used micro *in utero* electroporation (Matsui et al., 2011) to focally overexpress *EYFP* and the murine *Lhx9* ortholog, or *EYFP* alone, in the developing murine diencephalon at embryonic day (E) 10.5 and assayed *Hcrt* expression at postnatal day (P) 6. Embryos overexpressing *Lhx9* had significantly more *Hcrt*-expressing neurons in the lateral hypothalamus than embryos overexpressing *EYFP* alone (Fig. 8; supplementary material Figs S15 and S16). This effect appears to be specific, since *Lhx9* overexpression had no effect on the expression of other hypothalamic markers, including *Cartpt*, *Foxp2* and *Gal* (data not shown). *Lhx9* overexpression in the subthalamic zona incerta (supplementary material Fig. S17) or cerebral cortex (data not shown) did not induce ectopic *Hcrt* expression. We conclude that *Lhx9* is capable of promoting Hcrt neuron specification exclusively in its endogenous domain during mouse embryogenesis.

DISCUSSION

Using microarray gene expression analysis and high-throughput gene overexpression assays in zebrafish, we found that the LIM homeobox transcription factor Lhx9 is both necessary and sufficient to specify Hcrt neurons in zebrafish and is sufficient to specify Hcrt neurons in mouse embryos. We found that Lhx9 is also necessary and sufficient to specify QRFP neurons in zebrafish, which are located adjacent to Hcrt neurons in the hypothalamus. To our knowledge, this is the first study to identify a factor that is capable of inducing the specification of these neurons, or of any terminal neural subtype in the lateral hypothalamus.

Development (2015) 142, 1113-1124 doi:10.1242/dev.117424

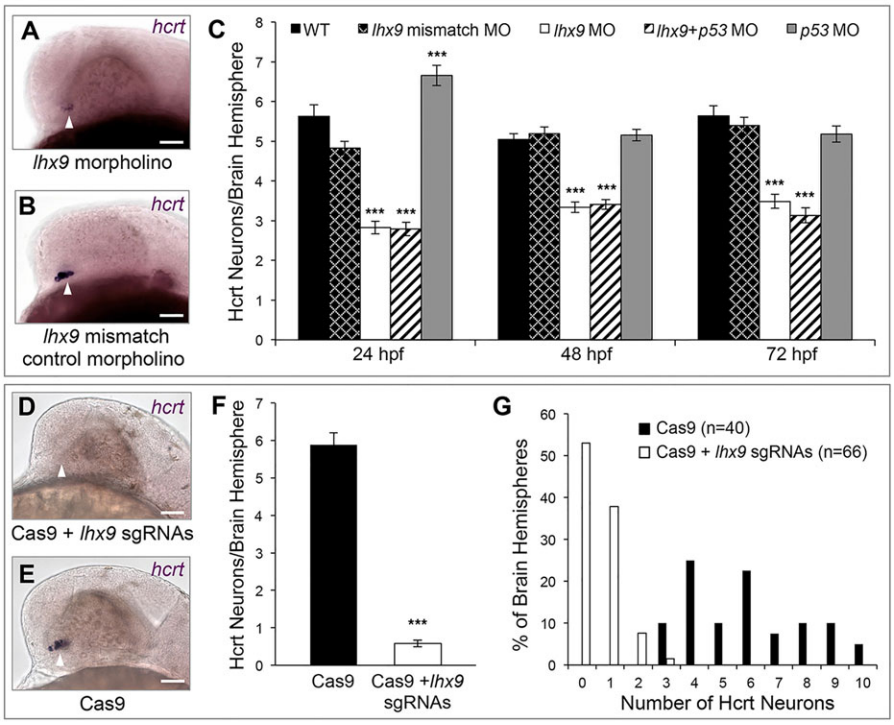

Fig. 6. Lhx9 is required for Hcrt neuron specification. (A-C) *hcrt* ISH at 24 hpf shows that morpholino-mediated knockdown of *lhx9* reduces the number of Hcrt neurons and the level of *hcrt* expression (A) compared with embryos injected with a control morpholino (B). (C) Quantification of Hcrt neurons per brain hemisphere at 24, 48 and 72 hpf revealed that *lhx9* morphants have ~40% fewer Hcrt neurons. Co-injecting a *p53* morpholino did not affect this phenotype. Mean±s.e.m. is shown. At least 22 embryos were quantified for each condition. ***P<0.001 compared with control morpholino (one-way ANOVA followed by Bonferroni's correction for multiple comparisons). (D-G) *hcrt* ISH at 24 hpf shows that co-injection of Cas9 protein and ten *lhx9* sgRNAs eliminates *hcrt* expression (D) compared with embryos injected with Cas9 alone (E). (F) Quantification of Hcrt neurons per brain hemisphere at 24 hpf. Mean±s.e.m. is shown. ***P<0.001 compared with Cas9 alone (one-way ANOVA). (G) The percentage of brain hemispheres containing the indicated number of Hcrt neurons. *n*, number of brain hemispheres analyzed in F,G. Arrowheads indicate endogenous Hcrt neuron region. Scale bars: 50 µm.

lhx9 was identified as enriched in Hcrt neurons by both our analysis of zebrafish embryos and by a previous study that used adult mice (Dalal et al., 2013). We analyzed zebrafish neurons just after the initiation of *hcrt* expression, enabling us to screen for transcripts that are likely to play a role in the specification of Hcrt neurons. We isolated purified cell populations by FACS, analyzed their gene expression patterns by microarray, and performed multiple pairwise comparisons of purified Hcrt neurons with a closely related cell type (QRFP-expressing neuron) and to more distantly related neurons (pan-neuronal or sensory neurons). By contrast, Dalal and colleagues used a translational profiling approach in which a tagged ribosomal subunit is expressed in Hcrt neurons. Biochemical purification of this subunit from a whole brain homogenate isolates transcripts that are actively translated in Hcrt neurons. Although this approach allowed profiling of the rare Hcrt cell population, its statistical power was diminished by contamination with nonspecific transcripts, as indicated by the presence of glial transcripts. In addition to *lhx9*, the 112 genes most enriched in Hcrt neurons in our study and the 188 most enriched genes identified by Dalal and colleagues include the definitive Hcrt neuron markers *hcrt* and *pdyn*, the transcription factors *hmx2* and *rfx4*, and *scg2*, *agrp*, *gliprl* and *fam46a*. The absence of more overlapping genes can be attributed in part to ambiguity in the gene assignment of microarray probes and the imperfect annotation of the zebrafish genome. Furthermore, the stringent criteria for significance used by both studies are likely to underestimate the true complement of Hcrt enriched genes shared between zebrafish embryos and adult mice.

Lhx9 belongs to the LIM homeobox family of transcription factors, which is conserved from invertebrates to mammals. These proteins have essential roles in tissue patterning and differentiation, particularly in the brain (Hobert and Westphal, 2000). In mice, several LIM homeobox proteins are expressed dynamically to demarcate regions of the developing hypothalamus (Shimogori et al., 2010). However, the developmental roles of specific LIM homeobox genes have been difficult to distinguish; loss-of-function phenotypes are subtle and similar LIM homeobox family members often exhibit redundancy. For instance, double knockdown of *lhx9* and *lhx2* dramatically altered thalamus and forebrain patterning in zebrafish, but knockdown of either gene alone had no gross effects (Peukert et al., 2011). Similarly, *Lhx9* knockout mice survive to adulthood without gross brain defects (Birk et al., 2000).

Although we tested morpholinos against several candidate genes, only the *lhx9* morpholino decreased the number of Hcrt neurons, with an average decrease of 40%. The remaining Hcrt neurons, which expressed *hcrt* at reduced levels, are likely to result from incomplete *lhx9* knockdown. Indeed, co-injection of Cas9 protein with sgRNAs targeting *lhx9* completely abolished *hcrt* expression in over half of brain hemispheres analyzed, indicating that *lhx9* is required for the specification of all Hcrt neurons. This result contrasts with *Lhx9* knockout mice, in which Hcrt neurons are only reduced by 39% (Dalal et al., 2013). This discrepancy is likely to be due to the expression of *lhx9* in all Hcrt neurons in zebrafish but in only a subset in mice (Shimogori et al., 2010).

In zebrafish, *lhx9* overexpression at 24 hpf was sufficient to produce ectopic Hcrt neurons in the medial hindbrain, but the number of Hcrt neurons in the hypothalamus remained unchanged. We characterized these ectopic Hcrt neurons at 120 hpf, when the Hcrt neuronal circuit is functional (Prober et al., 2006; Elbaz et al., 2012), and confirmed that all zebrafish Hcrt neurons in the hypothalamus and hindbrain express *pdyn* and *vglut1*, two markers of mammalian Hcrt neurons (Chou et al., 2001; Rosin et al., 2003). Unlike previous studies (Appelbaum et al., 2009; Rosin et al., 2003), we did not observe expression of *vglut2a* or *vglut2b* in hypothalamic or hindbrain Hcrt neurons, indicating that Hcrt neurons in larval zebrafish express different VGLUT family genes than adult zebrafish or rats. We also observed that all ectopic Hcrt neurons project to the LC, a target of Hcrt neurons in zebrafish and mammals (Horvath et al., 1999; Prober et al., 2006). Thus,

Development (2015) 142, 1113-1124 doi:10.1242/dev.117424

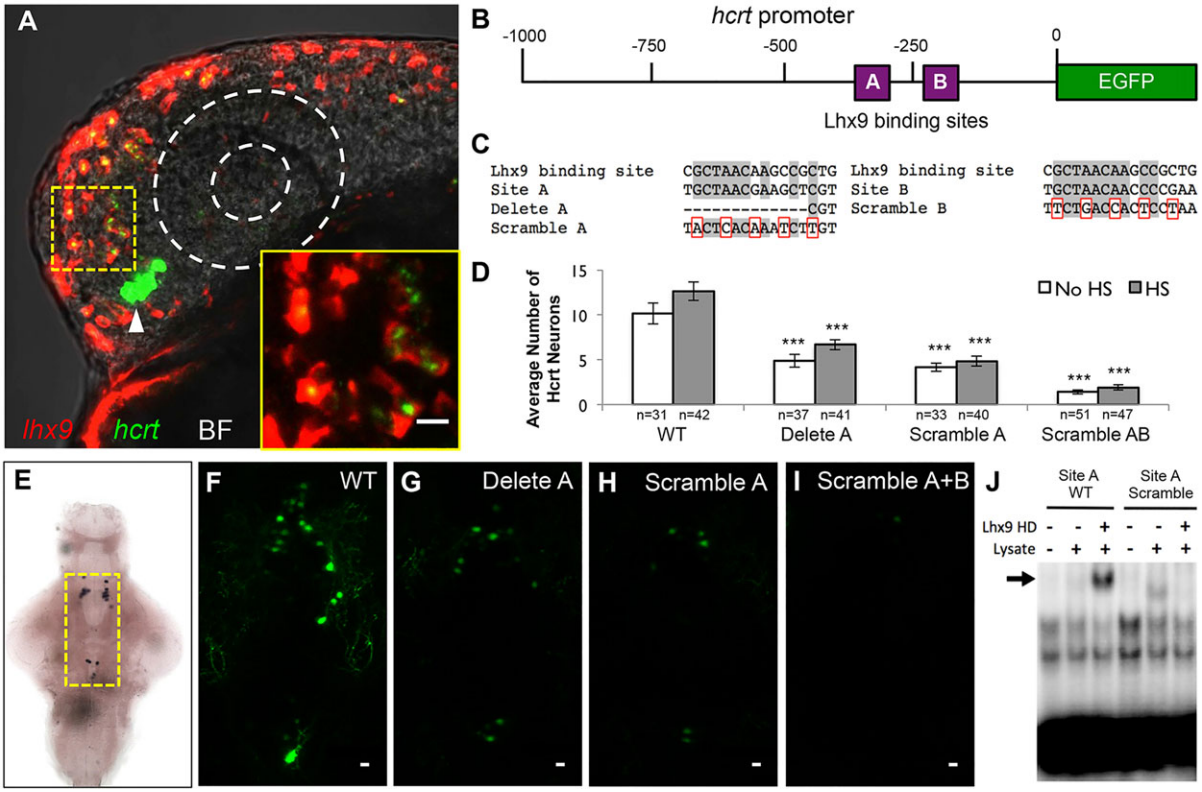

Fig. 7. Lhx9 can directly induce *hcrt* expression. (A) Ectopic *lhx9*-expressing neurons also express *hcrt* in embryos injected with an *hs:lhx9* plasmid, fixed 1 h after heat shock at 24 hpf, and analyzed using double fluorescent ISH with *hcrt*-specific and *lhx9*-specific probes. Arrowhead indicates endogenous Hcrt neurons. A single 1.5 µm confocal section is shown. Supplementary material Movie 4 contains the complete confocal image stack. The bright field (BF) overlay and dashed white circles show the position of the eye. The boxed region is shown at higher magnification in the inset. (B) Schematic of the zebrafish 1 kb *hcrt* promoter, including putative Lhx9 binding sites A and B. (C) Sequence of a previously characterized mammalian Lhx9 binding site compared with sites A and B in the zebrafish *hcrt* promoter and in mutated constructs. Gray shading, dashes and red boxes indicate conserved nucleotides, deleted nucleotides and mutated nucleotides, respectively. (D-I) Embryos were injected with a plasmid containing both *hcrt:EGFP* and *hs:lhx9*, and some injected embryos were heat-shocked at 24 hpf. Deletion or scrambling of putative Lhx9 binding sites reduced the number (D,F-I) and intensity (F-I) of EGFP-expressing cells. Cell counts indicate Hcrt cells per brain with (endogenous and ectopic Hcrt cells) and without (endogenous Hcrt cells only) heat shock. Mean±s.e.m. is shown. *n*, number of brains analyzed. ***P<0.001 compared with the wild-type promoter (one-way ANOVA followed by Bonferroni's correction for multiple comparisons). (E) Yellow box indicates area shown in F-I. (J) EMSA showing that the Lhx9 homeodomain (HD) binds to the wild-type (WT) site A (arrow), but not the scrambled site A, *in vitro*. Scale bars: 10 µm.

despite their location in the hindbrain, Lhx9-induced ectopic Hcrt neurons express the same genetic markers and project to the same target as endogenous Hcrt neurons.

Although it might be surprising that we did not detect an effect of *lhx9* overexpression on the number of hypothalamic Hcrt neurons, there are several possible explanations for this result. First, because *lhx9* induces few ectopic Hcrt neurons in our assay and the number of endogenous Hcrt neurons is variable, it is possible that *lhx9* induced additional Hcrt neurons in the hypothalamus but the difference was not large enough to detect. Second, endogenous *lhx9* is likely to act in concert with other factors to specify Hcrt neurons because only a subset of endogenous *lhx9*-expressing cells expresses *hcrt*. If these co-factors are only present in hypothalamic neurons that express endogenous *hcrt*, *lhx9* overexpression will have no effect on the number of Hcrt neurons in the hypothalamus. Other genes identified by our microarray analysis might encode these co-factors. However, overexpressing two or more candidate genes using our assay was not feasible due to DNA toxicity. Reducing the concentration of each injected plasmid to offset this toxicity also reduces the extent of gene overexpression. We were thus unable to observe ectopic Hcrt neurons when the *hs:lhx9* plasmid was co-injected with a second plasmid, and the number of hypothalamic Hcrt neurons was unaffected (data not shown).

We detected widespread co-expression of *lhx9* and *hcrt* 1 h after heat shock-induced *lhx9* overexpression. Because ectopic *hcrt* expression was observed so soon after heat shock, it seemed likely that Lhx9 was directly inducing *hcrt* expression. Consistent with this hypothesis, we identified two putative Lhx9 binding sites in the zebrafish *hcrt* promoter and found that they are necessary for both endogenous and ectopic *hcrt* expression *in vivo*. We also found that one binding site can form a complex with the Lhx9 homeodomain *in vitro*. However, this hypothesis is complicated by the fact that *lhx9* is widely expressed in the embryonic zebrafish brain, whereas *hcrt* is normally expressed exclusively in the hypothalamus. Because the extent of both *lhx9* overexpression and of ectopic *hcrt* expression is dramatically reduced by 24 h after heat shock (supplementary material Fig. S14), we propose that the ability of Lhx9 to drive *hcrt* expression may depend on Lhx9 levels. High Lhx9 levels might directly induce *hcrt* expression, whereas endogenous Lhx9 levels require one or more co-factors in the hypothalamus and medial hindbrain to promote and maintain *hcrt* expression.

Since the expression patterns of *hcrt* and *lhx9* are conserved between zebrafish and mammals (Peukert et al., 2011; Shimogori et al., 2010), we tested whether *Lhx9* overexpression could induce Hcrt neuron specification in mice. Indeed, *Lhx9* overexpression by

Development (2015) 142, 1113-1124 doi:10.1242/dev.117424

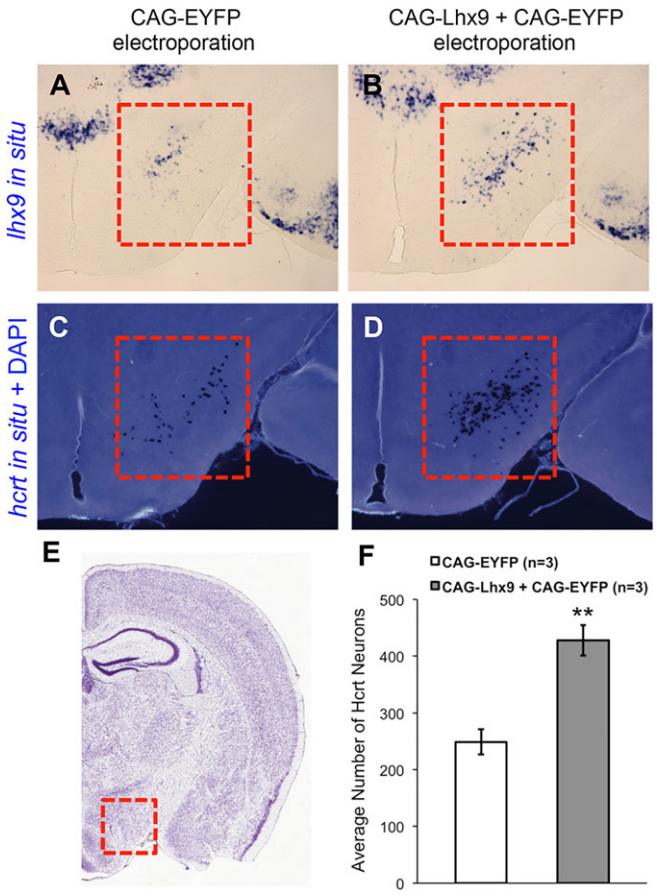

Fig. 8. *Lhx9* overexpression in mouse embryos promotes Hcrt neuron specification. (A-D) E10.5 mouse embryos were electroporated *in utero* into the right brain hemisphere lateral hypothalamus with either CAG-EYFP or with CAG-Lhx9+CAG-EYFP and analyzed at P6 for expression of *Lhx9* and *Hcrt* by ISH in serial coronal sections. Mice electroporated with CAG-Lhx9+CAG-EYFP have increased *Lhx9* expression (B) and more Hcrt cells (D) in the lateral hypothalamus (red boxes) than controls electroporated with CAG-EYFP alone (A,C). Coronal sections (A-D) are approximately Bregma −1.6 mm. (E) The entire right hemisphere of a comparable Nissl-stained section is shown for reference, with the red box indicating the lateral hypothalamus. Image adapted from the Allen Mouse Brain Atlas (Lein et al., 2006). (F) Quantification of Hcrt cell number in the lateral hypothalamus of the right brain hemisphere following electroporation with CAG-Lhx9+CAG-EYFP compared with CAG-EYFP alone. Mean±s.e.m. is shown for three experimental and three control brain hemispheres (see supplementary material Fig. S15 for quantification details). ***P*<0.01 (Student's *t*-test).

in utero electroporation was sufficient to specify additional Hcrt neurons, although they were only observed in the endogenous Hcrt neuron domain. This result suggests that the zone of cells competent to specify Hcrt neurons is more spatially restricted in mice than in zebrafish. Our findings differ from a previous study that saw no change in *Hcrt* expression after viral transduction of an *Lhx9*-overexpression construct in the hypothalamus of adult mice (Dalal et al., 2013). These results suggest that Lhx9 can induce Hcrt neuron specification in the embryonic, but not adult, mouse hypothalamus, possibly because cells competent to specify Hcrt neurons are fully differentiated in adults.

Our study demonstrates the utility of zebrafish to identify and test genes that regulate vertebrate development. Furthermore, the ability of Lhx9 to induce Hcrt neuron specification suggests a therapeutic approach to compensate for the loss of Hcrt neurons that is thought to cause narcolepsy. This strategy would use Lhx9 to generate *HCRT*-expressing neurons from human pluripotent stem cells *in vitro*, followed by screening and selection of Hcrt neurons to be transplanted into the hypothalamus. The promise of this approach is highlighted by the recent demonstration that narcoleptic-like sleep induced by the lesion of Hcrt neurons in rats is diminished by the transplantation of Hcrt neurons into the lateral hypothalamus (Arias-Carrión and Murillo-Rodríguez, 2014).

MATERIALS AND METHODS

Ethics statement

Zebrafish experiments followed standard protocols (Westerfield, 1993) in accordance with Caltech Institutional Animal Care and Use Committee guidelines. Mouse procedures were approved by the RIKEN Institutional Animal Care Committee.

Transgenic zebrafish

A 1-kb fragment of zebrafish genomic DNA upstream of *qrfp* was cloned upstream of *EGFP* using primers 5′-CTGACTCTCCCATCAGTCCT-3′ and 5′-CTGAAATTTAAGGAATAATTTAAAGTTG-3′. A 1-kb zebrafish genomic fragment upstream of *hcrt* (Faraco et al., 2006) was subcloned upstream of *mRFP* and *Kaede* using primers 5′-ATAATAAATAAAT-CTGATGGGGTTTT-3′ and 5′-GAGTTTAGCTTCTGTCCCCTG-3′. The *dbh:EGFP* transgene was generated by cloning a 1.1-kb fragment upstream of zebrafish *dbh* using primers 5′-ACTTGAACCAGCGACCTTCT-3′ and 5′-GGTTTGAAGGCCTTTCTAAGTTTTT-3′. Transgenes were co-injected with *tol2* transposase mRNA to generate stable transgenic lines. The *Tg(hcrt:EGFP)*, *Tg(elavl3:EGFP)*, *Tg(trpa1b:EGFP)*, *Tg(isl1:Gal4VP16, UAS:EGFP)*, *Tg(p2rx3b:EGFP)* and *Tg(vglut2a:RFP)* lines have been described (Prober et al., 2006; Park et al., 2000; Pan et al., 2012; Sagasti et al., 2005; Kucenas et al., 2006; Koyama et al., 2011). Hindbrain neurons were stochastically labeled by injecting a *Tg(elavl3:Kaede)* transgene (Sato et al., 2006).

Microarray analysis

We analyzed embryos co-expressing *qrfp:EGFP* and *hcrt:mRFP*, as well as separate transgenic lines expressing EGFP in all neurons [*Tg(elavl3:EGFP)*] or in subsets of sensory neurons [*Tg(trpa1b:EGFP)*, *Tg(isl1:Gal4VP16, 14xUAS:EGFP)*, *Tg(p2rx3b:EGFP)*]. Dechorionated embryos were anesthetized with tricaine at 26 hpf, incubated at room temperature in 0.25% trypsin-EDTA (Life Technologies) and manually dissociated. The cells were passed through a 40 µm strainer, pelleted and resuspended in cell culture medium for FACS (Manoli and Driever, 2012). Cells were incubated with Calcein Blue-AM (Life Technologies) to ensure the sorting of live cells. Sorting gates were set using wild-type embryos. Cells expressing EGFP or mRFP formed clear populations that were visually confirmed. Cells were sorted into a final volume of 100 µl PicoPure XB lysis buffer (Arcturus) and incubated at 42°C for 30 min. At least two independent sorting experiments were performed using each transgenic line. RNA was isolated (Arcturus PicoPure RNA, Life Technologies), amplified (MessageAmp II aRNA, Ambion) and quantified by bioanalyzer. cDNA libraries were prepared in duplicate or triplicate and labeled with Cy3 or Cy5 for hybridization to NimbleGen zv7 microarrays. Fluorophores were switched between replicates to minimize labeling bias. After scanning, data were normalized and pairwise comparisons were performed in R between Hcrt neurons and the five other sorted neuron populations. For each comparison, we generated a list of the most significantly Hcrt-enriched genes by intersecting the subset of probes that were at least fourfold upregulated in Hcrt neurons with the subset of probes with the most statistically significant differential expression using Bayesian statistics. The five pairwise comparisons were then intersected to identify probe sets consistently enriched in Hcrt neurons.

Zebrafish ISH and immunohistochemistry

Samples were fixed in 4% paraformaldehyde for 12-16 h at room temperature. ISH was performed using digoxigenin (DIG)-labeled antisense riboprobes (Thisse and Thisse, 2008). Images were acquired

Development (2015) 142, 1113-1124 doi:10.1242/dev.117424

using a Zeiss Axio ImagerM1 microscope. Fluorescent ISH used DIG- and 2,4-dinitrophenol (DNP)-labeled antisense riboprobes with the TSA Plus DNP System (PerkinElmer). Rabbit polyclonal anti-GFP (1:1000; MBL International, #598), rabbit polyclonal anti-orexin-A (Hcrt) (1:1000; Millipore, #AB3704) and goat anti-rabbit Alexa488 (1:500; Invitrogen, #A-11008) antibodies were used. Images were acquired using a Zeiss LSM 780 confocal microscope and analyzed using Fiji (Schindelin et al., 2012).

Candidate gene overexpression

The coding sequence of each candidate gene was amplified from 24 hpf zebrafish cDNA and cloned into pENTR-D-TOPO (Invitrogen). Gateway recombination (Invitrogen) was used to clone each gene downstream of a heat shock-inducible promoter (Halloran et al., 2000), and the entire cassette was flanked by Tol2 transposase sites. We co-injected individual overexpression plasmids with *tol2* transposase mRNA into zebrafish embryos at the 1-cell stage. Gene overexpression was induced by incubating embryos in a 37°C water bath for 1 h.

Morpholino-mediated knockdown

Morpholinos (GeneTools) were injected into wild-type embryos at the 1-cell stage. We used a splice-blocking morpholino to knock down Lhx9 (5′-AGCCTCAAAGTTAATGCTTACCTGT-3′). A morpholino with a 5 bp mismatch to the target was injected as a negative control (5′-AGCGTGAAACTTAATCCTTACCTCT-3′). Potential apoptosis was suppressed by co-injecting a *p53* morpholino (5′-GCGCCATTGCTTTGCAAGAATTG-3′). To verify knockdown efficacy, we isolated RNA from pools of five injected embryos and used RT-PCR (Superscript III First-Strand Synthesis System, Invitrogen) to amplify a fragment of the *lhx9* transcript that spans exon 2. To detect apoptosis, 24-hpf embryos were bathed in 1 µg/ml Acridine Orange for 1 h at room temperature, followed by three 10 min washes with E3 medium. Splice-blocking morpholinos were designed for *hmx2* (5′-TGGGAACGTCACTCACCGAGACAGA-3′) and *hmx3* (5′-TGCTGCTACAGTAATAGAGGCCAAA-3′) to retain the first intron of each gene, resulting in an early stop codon.

Quantitative reverse-transcription PCR (qRT-PCR)

We isolated total RNA from three biological replicates (25 embryos each) of *lhx9* morpholino-injected and control morpholino-injected embryos. TURBO DNase I was used to remove genomic DNA (TURBO DNA-free Kit, Invitrogen). We then generated cDNA (Superscript III First-Strand Synthesis System, Invitrogen) and amplified *hcrt* transcripts with primers 5′-GAGCATCAAGACTTTTCGATACA-3′ and 5′-ATGAAGACGAGCACCTGGAG-3′. Transcripts of the *rpl13a* reference gene were amplified with primers 5′-TCTGGAGGACTGTAAGAGGTATGC-3′ and 5′-AGACGCACAATCTTGAGAGCAG-3′. Each qRT-PCR reaction was run in triplicate on an ABI PRISM 7900HT Sequence Detection System (Applied Biosystems). Relative fold-change in expression was calculated using the $2^{-\Delta\Delta Ct}$ method (Schmittgen and Livak, 2008).

CRISPR/Cas9

Ten target sites within the *lhx9* open reading frame were chosen using CHOPCHOP (Montague et al., 2014) (supplementary material Table S2). Cas9 protein was mixed with all ten sgRNAs and injected into embryos at the 1-cell stage (Gagnon et al., 2014). At 24 hpf, deformed embryos were removed and the remainder were fixed in 4% paraformaldehyde for ISH. To control for potential sgRNA off-target effects, we co-injected Cas9 protein with independent subsets of the sgRNAs (subset 1 comprised sgRNAs 1, 3, 5, 7, 9; subset 2 comprised sgRNAs 2, 4, 6, 8, 10) (supplementary material Table S2).

hcrt enhancer constructs

We mutated one or both putative Lhx9 binding sites in the zebrafish *hcrt* promoter by PCR and Gibson assembly (Gibson et al., 2009). Enhancer fragments were placed upstream of the *EGFP* coding sequence. An *hs:lhx9* cassette was placed downstream of *hcrt*:*EGFP* in a vector containing Tol2 transposase sites.

Electrophoretic mobility shift assay (EMSA)

The following oligonucleotide probes (5′-3′) were used: site A wild-type probe, GTTGGTATTTGCTAACGAAGCTCGTCCTCCTGTCCA; site A scramble probe, GTTGGTATTTACTCACAAATCTTGTCCTCCTGTCCA; site B wild-type probe, TGACAAAGATGCTAACAACCCCGAAAAATCCTTTGT; site B scramble probe, TGACAAAGATTCTGACCACTCCTAAAAATCCTTTGT. Probes were radiolabeled using [γ-^{32}P]ATP and T4 polynucleotide kinase for 1 h at 37°C and column-purified (Illustra Microspin G-50, GE Healthcare). EMSAs were performed using a truncated form of zebrafish Lhx9 (Lhx9 HD) that contains the DNA-binding homeodomain but lacks both LIM domains (amino acids 224-396 of the 396 amino acid protein), as described (Wilhelm and Englert, 2002). Lhx9 HD was synthesized *in vitro* (TNT SP6 Quick Coupled Transcription/Translation System, Promega). 1 µl normalized radiolabeled oligo and 4.5 µl TNT lysate were added to a final volume of 30 µl binding buffer, containing 100 mM KCl, 1 mM $MgCl_2$, 10 µM $ZnSO_4$, 10 mM Tris pH 7.5, 4% glycerol, 1 mg/ml BSA, 200 ng poly(dIdC) and 0.5 mM DTT. After 1 h at room temperature, DNA-protein complexes were resolved by electrophoresis at 4°C on a 6% polyacrylamide DNA retardation gel (Invitrogen) at 100 V for 90 min in 0.5× TBE buffer. The gel was dried at 60°C for 2 h using a gel dryer (Bio-Rad) and analyzed by phosphorimaging (GE Healthcare).

Mouse experiments

Outbred ICR (CD-1) timed-pregnant mice were obtained from Japan SLC. Midday of the day of vaginal plug discovery was considered embryonic (E) day 0.5. Early postnatal mice were anesthetized with a lethal dose of pentobarbitone (100 mg/kg) and, after three failed attempts to elicit a foot withdrawal reflex, the animals were transcardially perfused with 4% paraformaldehyde in PBS. For ISH, brains were fixed overnight in 30% sucrose/4% paraformaldehyde and sectioned in the coronal plane on a Leica sledge microtome at 28 µm. Sections were mounted on slides and processed for non-radioactive ISH as described (Grove et al., 1998). DNA for riboprobes and electroporation were obtained from FANTOM clones (Carninci et al., 2005). Mouse *Lhx9* (GenBank NM_001025565) was subcloned into a CAG vector as described (Onishi et al., 2010) to generate an overexpression plasmid. *In utero* electroporation was performed as described (Matsui et al., 2011).

Acknowledgements

We thank Farhad Imam for assistance with microarray data analysis, Anthony Kirilushna for EMSA assistance and Daniel Lee for comments on the manuscript.

Competing interests

The authors declare no competing or financial interests.

Author contributions

D.A.P. and A.F.S. conceived and directed the project; J.L., F.T.M., J.A.G., T.S. and D.A.P. performed experiments; A.V.G. and C.N.C. generated and maintained reagents; I.G.W. provided microarray data; J.L., F.T.M., T.S., A.F.S. and D.A.P. wrote the paper.

Funding

This work was supported by grants from the National Institutes of Health [F31NS77844 to J.L.; 1R21NS071598, 5K99NS083713 to F.T.M.; R01HL109525, R21NS071598 to A.F.S.; R00NS060996, R01NS070911, R01DA031367 to D.A.P.], the American Cancer Society [to J.A.G. and I.G.W.], the Jane Coffin Childs Memorial Fund for Medical Research [to F.T.M.], the RIKEN Brain Institute [to T.S.], the Mallinckrodt Foundation, the Rita Allen Foundation, and the Brain and Behavior Research Foundation [to D.A.P.]. Deposited in PMC for release after 12 months.

Supplementary material

Supplementary material available online at
http://dev.biologists.org/lookup/suppl/doi:10.1242/dev.117424/-/DC1

References

Appelbaum, L., Wang, G. X., Maro, G. S., Mori, R., Tovin, A., Marin, W., Yokogawa, T., Kawakami, K., Smith, S. J., Gothilf, Y. et al. (2009). Sleep-wake regulation and hypocretin-melatonin interaction in zebrafish. *Proc. Natl. Acad. Sci. USA* **106**, 21942-21947.

Arias-Carrión, O. and Murillo-Rodríguez, E. (2014). Effects of hypocretin/orexin cell transplantation on narcoleptic-like sleep behavior in rats. *PLoS ONE* **9**, e95342.
Birk, O. S., Casiano, D. E., Wassif, C. A., Cogliati, T., Zhao, L., Zhao, Y., Grinberg, A., Huang, S., Kreidberg, J. A., Parker, K. L. et al. (2000). The LIM homeobox gene Lhx9 is essential for mouse gonad formation. *Nature* **403**, 909-913.
Blackshaw, S., Scholpp, S., Placzek, M., Ingraham, H., Simerly, R. and Shimogori, T. (2010). Molecular pathways controlling development of thalamus and hypothalamus: from neural specification to circuit formation. *J. Neurosci.* **30**, 14925-14930.
Bonnavion, P. and de Lecea, L. (2010). Hypocretins in the control of sleep and wakefulness. *Curr. Neurol. Neurosci. Rep.* **10**, 174-179.
Carninci, P., Kasukawa, T., Katayama, S., Gough, J., Frith, M. C., Maeda, N., Oyama, R., Ravasi, T., Lenhard, B., Wells, C. et al. (2005). The transcriptional landscape of the mammalian genome. *Science* **309**, 1559-1563.
Chartrel, N., Dujardin, C., Anouar, Y., Leprince, J., Decker, A., Clerens, S., Do-Régo, J.-C., Vandesande, F., Llorens-Cortes, C., Costentin, J. et al. (2003). Identification of 26RFa, a hypothalamic neuropeptide of the RFamide peptide family with orexigenic activity. *Proc. Natl. Acad. Sci. USA* **100**, 15247-15252.
Chiu, C. N. and Prober, D. A. (2013). Regulation of zebrafish sleep and arousal states: current and prospective approaches. *Front. Neural Circuits* **7**, 58.
Chou, T. C., Lee, C. E., Lu, J., Elmquist, J. K., Hara, J., Willie, J. T., Beuckmann, C. T., Chemelli, R. M., Sakurai, T., Yanagisawa, M. et al. (2001). Orexin (hypocretin) neurons contain dynorphin. *J. Neurosci.* **21**, RC168.
Cvetkovic-Lopes, V., Bayer, L., Dorsaz, S., Maret, S., Pradervand, S., Dauvilliers, Y., Lecendreux, M., Lammers, G.-J., Donjacour, C. E. H. M., Du Pasquier, R. A. et al. (2010). Elevated Tribbles homolog 2-specific antibody levels in narcolepsy patients. *J. Clin. Invest.* **120**, 713-719.
Dalal, J., Roh, J. H., Maloney, S. E., Akuffo, A., Shah, S., Yuan, H., Wamsley, B., Jones, W. B., Strong, C. d. G., Gray, P. A. et al. (2013). Translational profiling of hypocretin neurons identifies candidate molecules for sleep regulation. *Genes Dev.* **27**, 565-578.
Dauvilliers, Y., Arnulf, I. and Mignot, E. (2007). Narcolepsy with cataplexy. *Lancet* **369**, 499-511.
Elbaz, I., Yelin-Bekerman, L., Nicenboim, J., Vatine, G. and Appelbaum, L. (2012). Genetic ablation of hypocretin neurons alters behavioral state transitions in zebrafish. *J. Neurosci.* **32**, 12961-12972.
Elbaz, I., Foulkes, N. S., Gothilf, Y. and Appelbaum, L. (2013). Circadian clocks, rhythmic synaptic plasticity and the sleep-wake cycle in zebrafish. *Front. Neural Circuits* **7**, 9.
Faraco, J. H., Appelbaum, L., Marin, W., Gaus, S. E., Mourrain, P. and Mignot, E. (2006). Regulation of hypocretin (orexin) expression in embryonic zebrafish. *J. Biol. Chem.* **281**, 29753-29761.
Gagnon, J. A., Valen, E., Thyme, S. B., Huang, P., Ahkmetova, L., Pauli, A., Montague, T. G., Zimmerman, S., Richter, C. and Schier, A. F. (2014). Efficient mutagenesis by Cas9 protein-mediated oligonucleotide insertion and large-scale assessment of single-guide RNAs. *PLoS ONE* **9**, e98186.
Gibson, D. G., Young, L., Chuang, R.-Y., Venter, J. C., Hutchison, C. A. and Smith, H. O. (2009). Enzymatic assembly of DNA molecules up to several hundred kilobases. *Nat. Methods* **6**, 343-345.
Grove, E. A., Tole, S., Limon, J., Yip, L. and Ragsdale, C. W. (1998). The hem of the embryonic cerebral cortex is defined by the expression of multiple Wnt genes and is compromised in Gli3-deficient mice. *Development* **125**, 2315-2325.
Halloran, M. C., Sato-Maeda, M., Warren, J. T., Su, F., Lele, Z., Krone, P. H., Kuwada, J. Y. and Shoji, W. (2000). Laser-induced gene expression in specific cells of transgenic zebrafish. *Development* **127**, 1953-1960.
Hanisch, A., Holder, M. V., Choorapoikayil, S., Gajewski, M., Ozbudak, E. M. and Lewis, J. (2012). The elongation rate of RNA polymerase II in zebrafish and its significance in the somite segmentation clock. *Development* **140**, 444-453.
Higashijima, S., Hotta, Y. and Okamoto, H. (2000). Visualization of cranial motor neurons in live transgenic zebrafish expressing green fluorescent protein under the control of the islet-1 promoter/enhancer. *J. Neurosci.* **20**, 206-218.
Hobert, O. and Westphal, H. (2000). Functions of LIM-homeobox genes. *Trends Genet.* **16**, 75-83.
Honda, M., Eriksson, K. S., Zhang, S., Tanaka, S., Lin, L., Salehi, A., Hesla, P. E., Maehlen, J., Gaus, S. E., Yanagisawa, M. et al. (2009). IGFBP3 colocalizes with and regulates hypocretin (orexin). *PLoS ONE* **4**, e4254.
Horvath, T. L., Peyron, C., Diano, S., Ivanov, A., Aston-Jones, G., Kilduff, T. S. and van den Pol, A. N. (1999). Hypocretin (orexin) activation and synaptic innervation of the locus coeruleus noradrenergic system. *J. Comp. Neurol.* **415**, 145-159.
Hwang, W. Y., Fu, Y., Reyon, D., Maeder, M. L., Tsai, S. Q., Sander, J. D., Peterson, R. T., Yeh, J.-R. J. and Joung, J. K. (2013). Efficient genome editing in zebrafish using a CRISPR-Cas system. *Nat. Biotechnol.* **31**, 227-229.
Jao, L.-E., Wente, S. R. and Chen, W. (2013). Efficient multiplex biallelic zebrafish genome editing using a CRISPR nuclease system. *Proc. Natl. Acad. Sci. USA* **110**, 13904-13909.
Kaslin, J., Nystedt, J. M., Östergård, M., Peitsaro, N. and Panula, P. (2004). The orexin/hypocretin system in zebrafish is connected to the aminergic and cholinergic systems. *J. Neurosci.* **24**, 2678-2689.
Kosman, D., Mizutani, C. M., Lemons, D., Cox, W. G., McGinnis, W. and Bier, E. (2004). Multiplex detection of RNA expression in Drosophila embryos. *Science* **305**, 846.
Koyama, M., Kinkhabwala, A., Satou, C., Higashijima, S.-i. and Fetcho, J. (2011). Mapping a sensory-motor network onto a structural and functional ground plan in the hindbrain. *Proc. Natl. Acad. Sci. USA* **108**, 1170-1175.
Kucenas, S., Soto, F., Cox, J. A. and Voigt, M. M. (2006). Selective labeling of central and peripheral sensory neurons in the developing zebrafish using P2X3 receptor subunit transgenes. *Neuroscience* **138**, 641-652.
Lein, E. S., Hawrylycz, M. J., Ao, N., Ayres, M., Bensinger, A., Bernard, A., Boe, A. F., Boguski, M. S., Brockway, K. S., Byrnes, E. J. et al. (2006). Genome-wide atlas of gene expression in the adult mouse brain. *Nature* **445**, 168-176.
Machluf, Y., Gutnick, A. and Levkowitz, G. (2011). Development of the zebrafish hypothalamus. *Ann. N. Y. Acad. Sci.* **1220**, 93-105.
Manoli, M. and Driever, W. (2012). Fluorescence-activated cell sorting (FACS) of fluorescently tagged cells from zebrafish larvae for RNA isolation. *Cold Spring Harb. Protoc.* **2012**, ppii: pdb.prot069633.
Matsui, A., Yoshida, A. C., Kubota, M., Ogawa, M. and Shimogori, T. (2011). Mouse in utero electroporation: controlled spatiotemporal gene transfection. *J. Vis. Exp.* e3024.
Montague, T. G., Cruz, J. M., Gagnon, J. A., Church, G. M. and Valen, E. (2014). CHOPCHOP: a CRISPR/Cas9 and TALEN web tool for genome editing. *Nucleic Acids Res.* **42**, W401-W407.
Onishi, A., Peng, G.-H., Poth, E. M., Lee, D. A., Chen, J., Alexis, U., de Melo, J., Chen, S. and Blackshaw, S. (2010). The orphan nuclear hormone receptor ERRβ controls rod photoreceptor survival. *Proc. Natl. Acad. Sci. USA* **107**, 11579-11584.
Pan, Y. A., Choy, M., Prober, D. A. and Schier, A. F. (2012). Robo2 determines subtype-specific axonal projections of trigeminal sensory neurons. *Development* **139**, 591-600.
Park, H.-C., Kim, C.-H., Bae, Y.-K., Yeo, S.-Y., Kim, S.-H., Hong, S.-K., Shin, J., Yoo, K.-W., Hibi, M., Hirano, T. et al. (2000). Analysis of upstream elements in the HuC promoter leads to the establishment of transgenic zebrafish with fluorescent neurons. *Dev. Biol.* **227**, 279-293.
Peukert, D., Weber, S., Lumsden, A. and Scholpp, S. (2011). Lhx2 and Lhx9 determine neuronal differentiation and compartition in the caudal forebrain by regulating Wnt signaling. *PLoS Biol.* **9**, e1001218.
Peyron, C., Faraco, J., Rogers, W., Ripley, B., Overeem, S., Charnay, Y., Nevsimalova, S., Aldrich, M., Reynolds, D., Albin, R. et al. (2000). A mutation in a case of early onset narcolepsy and a generalized absence of hypocretin peptides in human narcoleptic brains. *Nat. Med.* **6**, 991-997.
Prober, D. A., Rihel, J., Onah, A. A., Sung, R.-J. and Schier, A. F. (2006). Hypocretin/orexin overexpression induces an insomnia-like phenotype in zebrafish. *J. Neurosci.* **26**, 13400-13410.
Prober, D. A., Zimmerman, S., Myers, B. R., McDermott, B. M., Kim, S.-H., Caron, S., Rihel, J., Solnica-Krezel, L., Julius, D., Hudspeth, A. J. et al. (2008). Zebrafish TRPA1 channels are required for chemosensation but not for thermosensation or mechanosensory hair cell function. *J. Neurosci.* **28**, 10102-10110.
Robu, M. E., Larson, J. D., Nasevicius, A., Beiraghi, S., Brenner, C., Farber, S. A. and Ekker, S. C. (2007). p53 activation by knockdown technologies. *PLoS Genet.* **3**, e78.
Rosin, D. L., Weston, M. C., Sevigny, C. P., Stornetta, R. L. and Guyenet, P. G. (2003). Hypothalamic orexin (hypocretin) neurons express vesicular glutamate transporters VGLUT1 or VGLUT2. *J. Comp. Neurol.* **465**, 593-603.
Sagasti, A., Guido, M. R., Raible, D. W. and Schier, A. F. (2005). Repulsive interactions shape the morphologies and functional arrangement of zebrafish peripheral sensory arbors. *Curr. Biol.* **15**, 804-814.
Sato, T., Takahoko, M. and Okamoto, H. (2006). HuC:Kaede, a useful tool to label neural morphologies in networks in vivo. *Genesis* **44**, 136-142.
Sawai, N., Ueta, Y., Nakazato, M. and Ozawa, H. (2010). Developmental and aging change of orexin-A and -B immunoreactive neurons in the male rat hypothalamus. *Neurosci. Lett.* **468**, 51-55.
Schindelin, J., Arganda-Carreras, I., Frise, E., Kaynig, V., Longair, M., Pietzsch, T., Preibisch, S., Rueden, C., Saalfeld, S., Schmid, B. et al. (2012). Fiji: an open-source platform for biological-image analysis. *Nat. Methods* **9**, 676-682.
Schmittgen, T. D. and Livak, K. J. (2008). Analyzing real-time PCR data by the comparative CT method. *Nat. Protoc.* **3**, 1101-1108.
Shimogori, T., Lee, D. A., Miranda-Angulo, A., Yang, Y., Wang, H., Jiang, L., Yoshida, A. C., Kataoka, A., Mashiko, H., Avetisyan, M. et al. (2010). A genomic atlas of mouse hypothalamic development. *Nat. Neurosci.* **13**, 767-775.
Takayasu, S., Sakurai, T., Iwasaki, S., Teranishi, H., Yamanaka, A., Williams, S. C., Iguchi, H., Kawasawa, Y. I., Ikeda, Y., Sakakibara, I. et al. (2006). A neuropeptide ligand of the G protein-coupled receptor GPR103 regulates feeding, behavioral arousal, and blood pressure in mice. *Proc. Natl. Acad. Sci. USA* **103**, 7438-7443.

Development (2015) 142, 1113-1124 doi:10.1242/dev.117424

Tessmar-Raible, K., Raible, F., Christodoulou, F., Guy, K., Rembold, M., Hausen, H. and Arendt, D. (2007). Conserved sensory-neurosecretory cell types in annelid and fish forebrain: insights into hypothalamus evolution. *Cell* **129**, 1389-1400.

Thannickal, T. C., Moore, R. Y., Nienhuis, R., Ramanathan, L., Gulyani, S., Aldrich, M., Cornford, M. and Siegel, J. M. (2000). Reduced number of hypocretin neurons in human narcolepsy. *Neuron* **27**, 469-474.

Thisse, C. and Thisse, B. (2008). High-resolution in situ hybridization to whole-mount zebrafish embryos. *Nat. Protoc.* **3**, 59-69.

Tsujino, N. and Sakurai, T. (2009). Orexin/hypocretin: a neuropeptide at the interface of sleep, energy homeostasis, and reward system. *Pharmacol. Rev.* **61**, 162-176.

Westerfield, M. (1993). *The Zebrafish Book. A Guide for The Laboratory Use of Zebrafish (Danio rerio)*, 4th edn. Eugene, OR: University of Oregon Press.

Wilhelm, D. and Englert, C. (2002). The Wilms tumor suppressor WT1 regulates early gonad development by activation of Sf1. *Genes Dev.* **16**, 1839-1851.

Wilson, S. W. and Houart, C. (2004). Early steps in the development of the forebrain. *Dev. Cell* **6**, 167-181.

Yamamoto, T., Miyazaki, R. and Yamada, T. (2009). Intracerebroventricular administration of 26RFa produces an analgesic effect in the rat formalin test. *Peptides* **30**, 1683-1688.

Figure S1. Validation of zebrafish QRFP, Hcrt, and DBH transgenic reporter lines. All cells labeled by fluorescent ISH for *qrfp* and *dbh* are also labeled by anti-GFP immunostaining in *Tg(qrfp:EGFP, hcrt:mRFP)* embryos at 24 hpf (A) and *Tg(dbh:EGFP)* larvae at 120 hpf (C). All mRFP expressing cells in 24 hpf *Tg(qrfp:EGFP, hcrt:mRFP)* embryos are labeled by anti-Hcrt immunostaining (B). Anterior (A,B) and dorsal (C) views are shown. Scale = 10 μm.

Figure S2. Strategy to identify genes enriched in embryonic zebrafish Hcrt neurons. Transgenic zebrafish embryos were dissociated into single cells at 26 hpf and cells of interest were purified by FACS. RNA from purified neurons was amplified and hybridized to microarrays. Signals from Hcrt neurons were compared to other neuron types and genes most highly enriched in Hcrt neurons were identified. Highly enriched transcription factors and secreted peptides were selected for verification by ISH and overexpression analysis in zebrafish.

Figure S3. Expression patterns of genes identified as enriched in Hcrt neurons. ISH was performed using wild-type zebrafish embryos at 24 hpf. Anterior is left. Most candidate genes are expressed in a domain that is similar to, or overlaps with, the *hcrt* expression domain. Images in the bottom row were obtained from the ZFIN ISH database (Liu and Patient, 2008; Thisse et al., 2004).

Figure S4. Time course of endogenous *hcrt* and *lhx9* expression. Confocal projections of *Tg(hcrt:EGFP)* embryos at 24, 48, 72, 96, and 120 hpf show that all Hcrt cells express

lhx9 throughout development, as determined by fluorescent ISH for *lhx9* followed by anti-GFP immunostaining. Ventral images are shown. Scale = 10 μm.

Figure S5. Overexpression of candidate genes does not affect the number of Hcrt neurons in the hypothalamus. Overexpression of each candidate gene was induced by heat shock at 24 hpf and larvae were fixed at 120 hpf for ISH with a *hcrt* probe. Mean ± s.e.m. number of Hcrt cells in the entire hypothalamus is shown. Control larvae were injected with a HS-EGFP plasmid. n indicates number of larval brains analyzed. No significant difference was detected between any overexpressed gene and control ($p>0.05$ by one-way ANOVA). Note that ectopic Hcrt neurons (i.e. not in the hypothalamus) were only observed following overexpression of *lhx9* (Fig. 3).

Figure S6. *lhx9* overexpression induces ectopic QRFP neurons. (A-D) Ectopic *qrfp:EGFP* expressing neurons that persist until 96 hours post HS (120 hpf) also express ectopic *lhx9* (arrowheads in C, D). (E-H) Double fluorescent ISH for *lhx9* and *qrfp* in WT 120 hpf larvae shows an absence of *lhx9* expression in the hindbrain region that contains *lhx9*-induced ectopic *qrfp* neurons in (A-D). Boxed regions in (A, B, E, F) are shown at higher magnification in (C, D, G, H). (A, B, E, F) show 95 μm thick confocal maximum intensity projections containing both endogenous and ectopic QRFP neurons. (C, D, G, H) show 43 μm thick confocal maximum intensity projections including only the region containing ectopic QRFP neurons. *lhx9*-expressing neurons that appear close to ectopic QRFP neurons in (B) are located 30 μm ventral to the ectopic QRFP neurons, and are thus not observed in (D). Scale = 10 μm.

Figure S7. Expression of endogenous *qrfp* and *lhx9*. Confocal projections of WT embryos at 24 and 120 hpf show that all *qrfp*-expressing cells express *lhx9*, as determined by double fluorescent ISH. Ventral images are shown. Scale = 10 μm.

Figure S8. Hcrt neurons do not express *vglut2a* at 120 hpf. Confocal projections of a 120 hpf *Tg(vglut2a:mRFP, hcrt:EGFP)* larva shows that *vglut2a* cells labeled with mRFP do not colocalize with endogenous (A) or ectopic (C) Hcrt neurons labeled with EGFP. The regions shown in (A) and (C) are indicated with dashed boxes in (B) and (D), respectively. Scale = 10 μm.

Figure S9. Few or no Hcrt neurons express *vglut2b* at 120 hpf. Confocal projections of a 120 hpf *Tg(hcrt:EGFP)* larva shows that most Hcrt neurons immunostained with a GFP-specific antibody do not co-localize with *vglut2b*-expressing cells labeled by fluorescent ISH. Weak co-labeling was occasionally observed in endogenous and ectopic Hcrt neurons (white arrowheads). The approximate regions shown in (A) and (C) are indicated with dashed boxes in (B) and (D), respectively. Scale = 10 μm.

Figure S10. Molecular analysis of *lhx9* morpholino knockdown. (A) Mature *lhx9* mRNA lacks part or all of the second exon after injection with a splice blocking morpholino, reducing the PCR product size by 96 bp or 203 bp, respectively. A 5 bp mismatch control morpholino and the apoptosis suppressing p53 morpholino have no effect on *lhx9* splicing. Gene knockdown persists until at least 72 hpf. Note that a small

amount of correctly spliced *lhx9* is present at all time points, indicating incomplete knockdown. (B) Diagram of the five exons of wild-type *lhx9* and the two variants caused by the *lhx9* morpholino. A cryptic splice site in exon 2 produces an in-frame 32 amino acid deletion that removes most of the LIM1 domain (Band 2). A second variant (Band 3) lacks exon 2, contains an early stop codon and lacks both LIM domains and the DNA-binding homeodomain (HD).

Figure S11. Endogenous *hcrt*- and *pdyn*-expressing neurons are reduced in *lhx9* morphants. *Tg(hcrt:EGFP)* embryos injected with either *lhx9* morpholino (C, D) or *lhx9* mismatch control morpholino (A, B) were fixed at 72 hpf and probed for *vglut1* or *pdyn* expression by fluorescent ISH. No obvious defects in *vglut1* expression were observed in *lhx9* morphants, but the total number of cells with intense, punctate *pdyn* expression was reduced by approximately 40% (E). This result suggests that the morpholino-induced reduction in Hcrt neurons is caused by cell loss, rather than silencing of *hcrt* expression. n indicates number of morphant brains analyzed. ***, $p<0.001$ compared to embryos injected with the control morpholino by Student's t-test. Scale = 10 μm.

Figure S12. The *lhx9* morpholino does not induce apoptosis and can be rescued by *lhx9* overexpression. *Tg(hcrt:mRFP)* embryos were stained with acridine orange at 24 hpf to quantify apoptotic cells (A-D). There was no increase in apoptosis in embryos injected with *lhx9* morpholino (C) compared to embryos injected with the *lhx9* mismatch control morpholino (B) or wild-type embryos (A), suggesting that the reduced number of Hcrt neurons in *lhx9* morphants is not due to apoptosis. Acridine orange labeled fewer

cells in embryos injected with the p53 morpholino (D), presumably because apoptosis that normally occurs during development was suppressed. (E) Mean ± s.e.m. number of apoptotic cells in the white boxed region. At least 4 embryo brains were analyzed for each condition. **, $p<0.01$ compared to WT by one-way ANOVA followed by Bonferroni's correction for multiple comparisons. (F) To rescue the morpholino phenotype, *Tg(hcrt:EGFP)* embryos were co-injected with the *lhx9* morpholino and the *hs:lhx9* plasmid. Following heat shock at 24 hpf, *lhx9*-overexpressing cells located in the endogenous *hcrt* expression domain also expressed *hcrt* (white arrowheads), indicating that *lhx9* overexpression can rescue the *lhx9* morpholino phenotype. (G) Mean ± s.e.m. number of endogenous and rescued *hcrt* cells per brain. Following rescue, the total number of *hcrt*-expressing cells is similar to the number observed in wild-type embryo brains (see Fig. 2G). *hcrt* expression in rescued cells was weaker than in endogenous Hcrt neurons, presumably because the rescued cells only received a pulse of *lhx9* while endogenous Hcrt neurons continuously express *lhx9*. Three embryo brains with ectopic *lhx9* expression in the endogenous Hcrt region were quantified. Anterior views of 26 hpf embryos are shown. Scale = 10 μm.

Figure S13. CRISPR/Cas9 targeting of *lhx9* affects Hcrt and QRFP neuron specification. (A) Embryos injected with Cas9+*lhx9* sgRNA subset 1 (sgRNAs 1, 3, 5, 7, 9) or Cas9+*lhx9* sgRNA subset 2 (sgRNAs 2, 4, 6, 8, 10) (supplementary material Table S2) show a 5.1-fold and 3.7-fold reduction, respectively, in the number of Hcrt neurons per brain hemisphere compared to embryos injected with Cas9 alone. (C) Embryos injected with Cas9 and all 10 *lhx9* sgRNAs show a 2.7-fold reduction in the number of

QRFP neurons per brain hemisphere. This reduction was significant, but less dramatic than the reduction observed for Hcrt neurons (Fig. 6F). (E) Embryos injected with Cas9+*lhx9* sgRNA subset 1 or Cas9+*lhx9* sgRNA subset 2 have significantly fewer QRFP neurons in each brain hemisphere. Injection of the two non-overlapping *lhx9* sgRNA subsets each causes the same phenotype as injection of all 10 sgRNAs, suggesting that loss of Hcrt and QRFP cells is due to *lhx9* knockout and not due to off-target effects of particular sgRNAs. Histograms in (B, D, F) show the percentage of brain hemispheres containing the indicated number of Hcrt neurons measured in (A, C, E). ***, $p<0.001$ compared to control embryos injected with Cas9 alone by one-way ANOVA followed by Tukey's correction for multiple comparisons. n indicates number of brain hemispheres analyzed.

Figure S14. Time course of *lhx9* and *hcrt* expression after heat shock.

Double fluorescent ISH for *lhx9* and *hcrt* are shown at 1 hour, 8 hours, and 24 hours after heat shock (HS)-induced *lhx9* overexpression. Fluorescent ISH for *lhx9* and immunostained *hcrt:EGFP* is shown at 96 hours post HS. (B) At 1 hour post HS, widespread *lhx9* mRNA is detected throughout the embryo. Nearly all *lhx9*-expressing cells also express *hcrt*. (D) At 8 hours post HS, the number of cells with *lhx9* overexpression and ectopic *hcrt* expression is reduced by approximately four-fold. Most *lhx9*-expressing cells still express *hcrt*. (F) At 24 hours post HS, little ectopic *lhx9* or *hcrt* expression is observed, except for ectopic *lhx9*- and *hcrt*-co-expressing neurons in the medial hindbrain. Ectopic *hcrt*-expressing neurons that persist until 96 hours post HS (120 hpf) also express ectopic *lhx9* (H, J). In contrast, control embryos injected with

empty heat shock vector only exhibit *hcrt* expression in the hypothalamus (A, C, E, G, I). Arrowheads indicate examples of ectopic *lhx9* and *hcrt* co-expression. (G, H) show 91 μm thick confocal maximum intensity projections containing both endogenous and ectopic Hcrt neurons. (I, J) show 45 μm thick confocal maximum intensity projections including only the region containing ectopic Hcrt neurons. *lhx9*-expressing neurons that appear close to ectopic Hcrt neurons in (H) are located 30 μm ventral to the ectopic Hcrt neurons, and are thus not observed in (J). Embryos fixed at 1 hour and 8 hours post HS are shown in side view. Embryos fixed at 24 hours and 96 hours post HS are shown dorsally and ventrally, respectively. Boxed regions in (G, H) are shown at higher magnification in (I, J). Scale indicates 50 μm (A-F) and 10 μm (G-J).

Figure S15. Quantification of Hcrt neuron specification following *in utero* overexpression of *lhx9*. E10.5 mouse embryos were electroporated with CAG-EYFP (A) or CAG-Lhx9 + CAG-EYFP (B) *in utero* into the right brain hemisphere lateral hypothalamus and analyzed at P6 for *hcrt* expression by ISH in 6 adjacent coronal sections. Sections were co-stained with DAPI to visualize individual cells to facilitate accurate quantification of *hcrt* ISH (DAPI co-stain is shown for all three brains in (A) and for two brains in (B)). White dots in (A) are included to show how quantification was performed. White numbers indicate the number of *hcrt*-expressing neurons in a brain hemisphere in each section. (C) Mean ± s.e.m. number of *hcrt*-expressing neurons for three experimental and three control brain hemispheres in each section. *, $p<0.05$ compared to control by Student's t-test. These data were combined to generate the graph in Fig. 8F.

Figure S16. Hypothalamic *lhx9* overexpression coincides with increased *hcrt*-expressing neurons. Six serial coronal sections of exemplar brains electroporated with CAG-EYFP or CAG-Lhx9 + CAG-EYFP in the right brain hemisphere lateral hypothalamus at E10.5 and processed for *hcrt* (A) or *lhx9* (B) ISH at P6 are shown. *hcrt* ISH sections were co-stained with DAPI to facilitate quantification of *hcrt*-expressing neurons. The majority of ectopic *lhx9*-expressing neurons are observed in sections 4 and 5 (B, compare boxed region in right column to left column), which coincides with sections that show the greatest increase in *hcrt*-expressing neurons compared to CAG-EYFP controls (A, compare boxed regions in right column to left column). See Fig. S12 for quantification of *hcrt*-expressing neurons in each section. The CAG-EYFP and CAG-Lhx9 + CAG-EYFP images shown are the same as brain 2 and brain 1 in Fig. S12, respectively.

Figure S17. *lhx9* overexpression in the zona incerta does not induce Hcrt neuron specification. Mice electroporated with CAG-Lhx9 + CAG-EYFP in the zona incerta (ZI) (A, red arrow), show no ectopic Hcrt neurons in the ZI (B). *hcrt* ISH was allowed to develop longer for these samples than those shown in Figs 8, S12 and S13 to ensure that any faint *hcrt* expression in the ZI could be detected. Dashed box indicates the lateral hypothalamus.

Table S1. Genes identified by microarray as enriched in Hcrt neurons. This table contains three sheets containing processed microarray data used to identify Hcrt enriched

genes. Sheet 1: Alphabetized list of the genes enriched in Hcrt neurons in multiple pair-wise comparisons. Sheet 2: Summary of data used to generate the gene list in Sheet 1, including probe name, the number of pair-wise comparisons for which a probe reached significance, the significance rank for a probe in each comparison, and detailed information on the gene represented by a probe. Sheet 3: R analysis used to obtain Sheet 2. Each probe was independently ranked by fold change and Bayesian significance and the combined P value was computed and adjusted. Raw data used to generate the values in Sheet 3 are available upon request. Note that the microarray did not contain probes for QRFP.

Table S2. sgRNAs used to target *lhx9* using the CRISPR/Cas9 system. This table lists the sequences of the 10 sgRNAs used to target *lhx9* using CRISPR/Cas9.

Supplementary References

Liu, F. and Patient, R. (2008). Genome-wide analysis of the zebrafish ETS family identifies three genes required for hemangioblast differentiation or angiogenesis. *Circ. Res.* **103**, 1147–1154.

Thisse, B., Heyer, V., Lux, A., Alunni, V., Degrave, A., Seiliez, I., Kirchner, J., Parkhill, J.-P. and Thisse, C. (2004). Spatial and temporal expression of the zebrafish genome by large-scale in situ hybridization screening. *Methods Cell Biol.* **77**, 505–519.

Figure S1

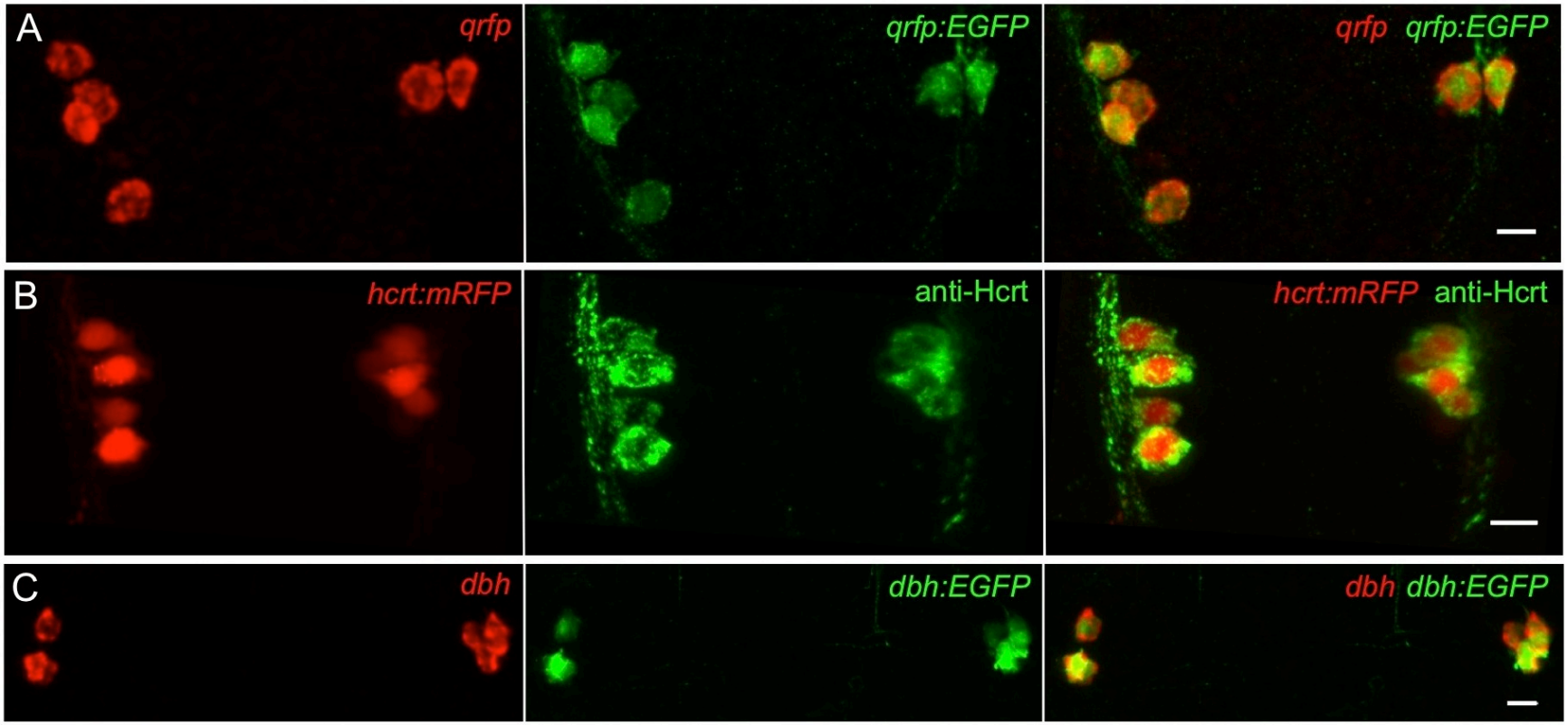
A
qrfp
qrfp:EGFP
qrfp qrfp:EGFP
B
hcrt:mRFP
anti-Hcrt
hcrt:mRFP anti-Hcrt
C
dbh
dbh:EGFP
dbh dbh:EGFP

Figure S2

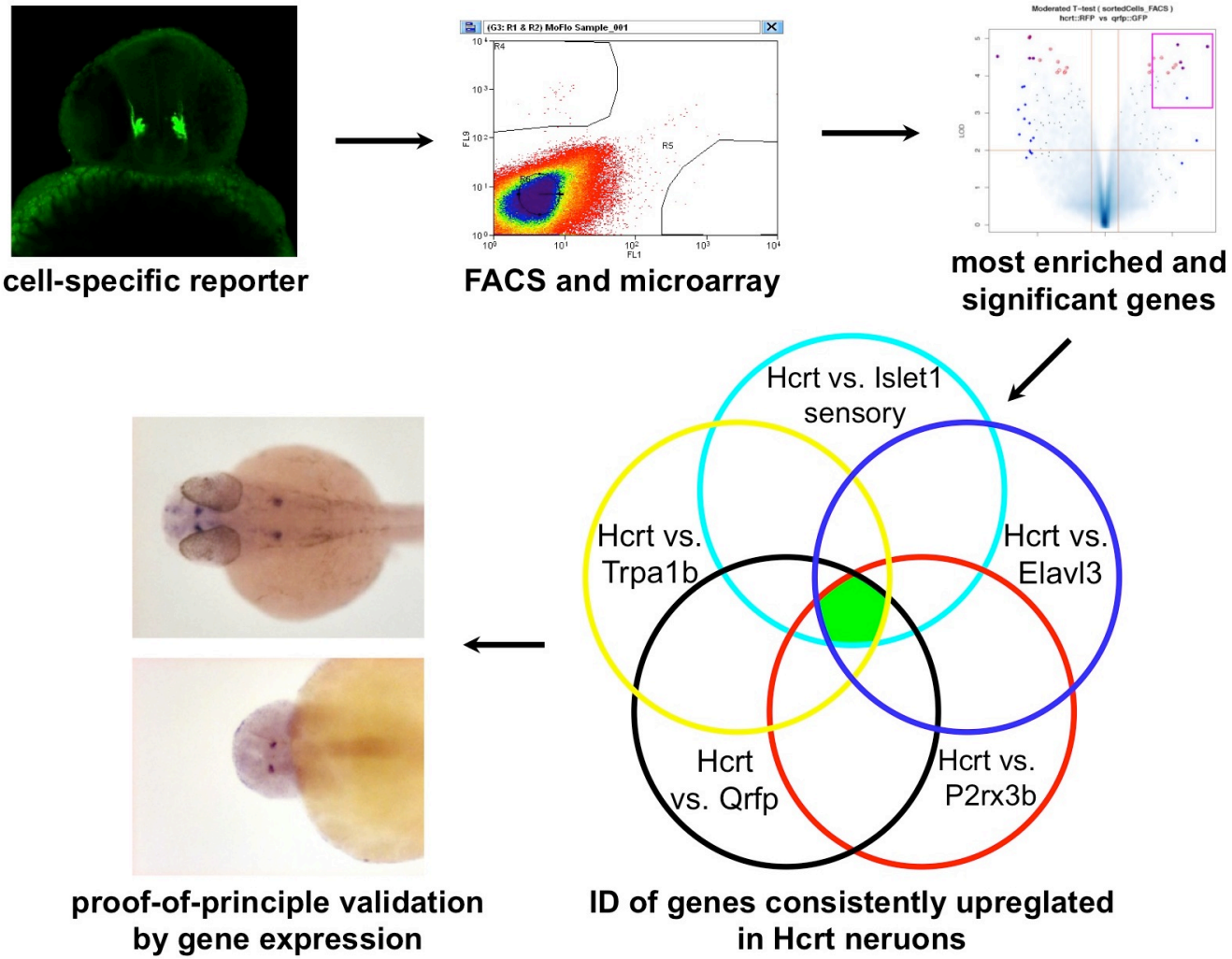
cell-specific reporter
FACS and microarray
most enriched and
significant genes
Hcrt vs. Islet1
sensory
Hcrt vs.
Trpa1b
Hcrt vs.
Elavl3
Hcrt
vs. Qrfp
Hcrt vs.
P2rx3b
proof-of-principle validation
by gene expression
ID of genes consistently upreglated
in Hcrt neruons

Figure S3

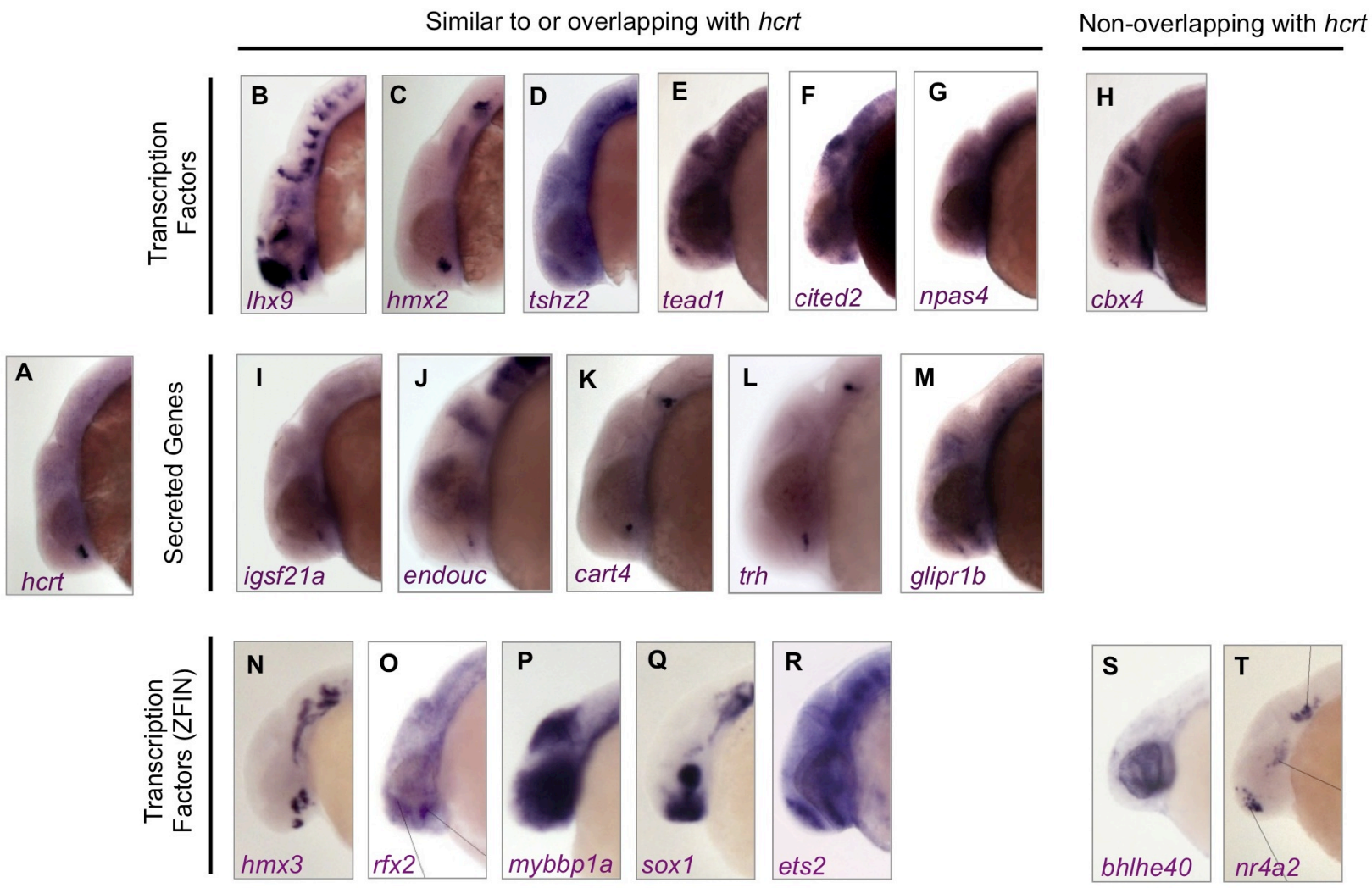
Similar to or overlapping with *hcrt*
Non-overlapping with *hcrt*
Transcription Factors
Secreted Genes
Transcription Factors (ZFIN)
A
hcrt
B
lhx9
C
hmx2
D
tshz2
E
tead1
F
cited2
G
npas4
H
cbx4
I
igsf21a
J
endouc
K
cart4
L
trh
M
glipr1b
N
hmx3
O
rfx2
P
mybbp1a
Q
sox1
R
ets2
S
bhlhe40
T
nr4a2

Figure S4

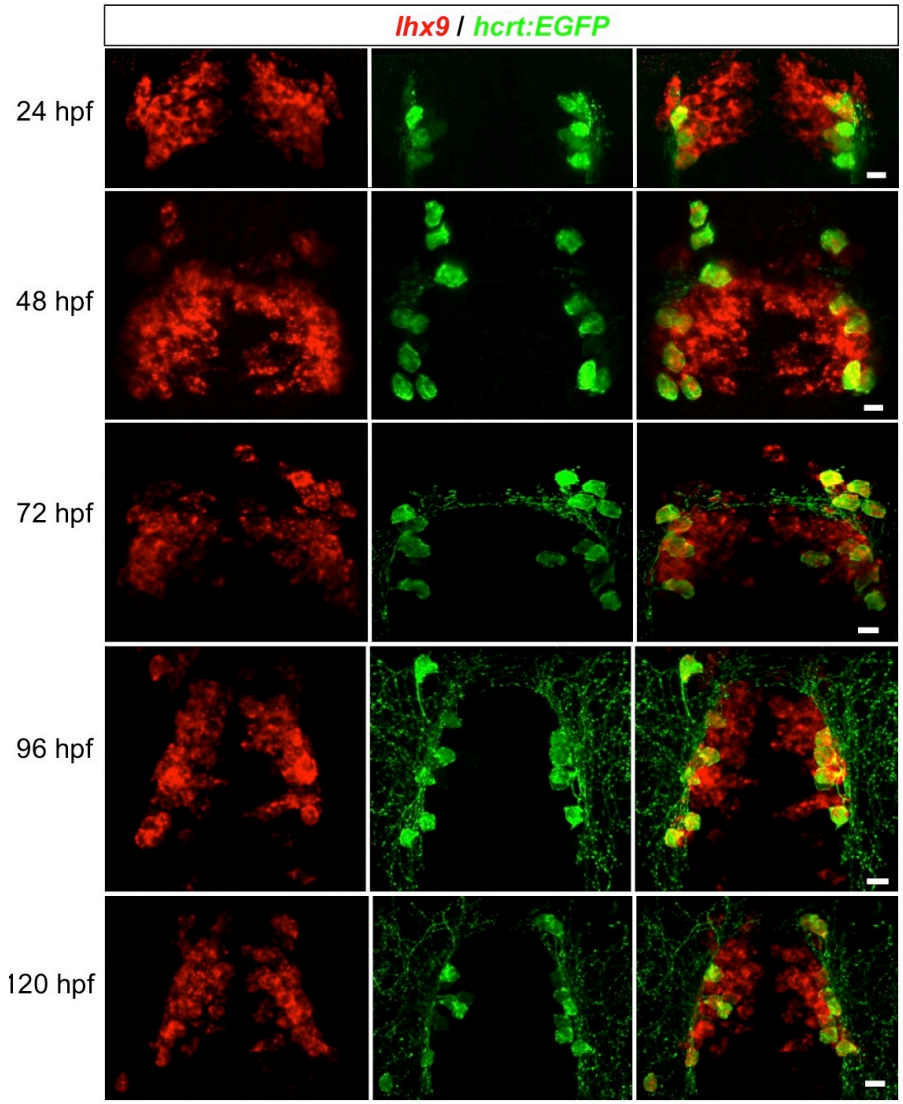

Figure S5

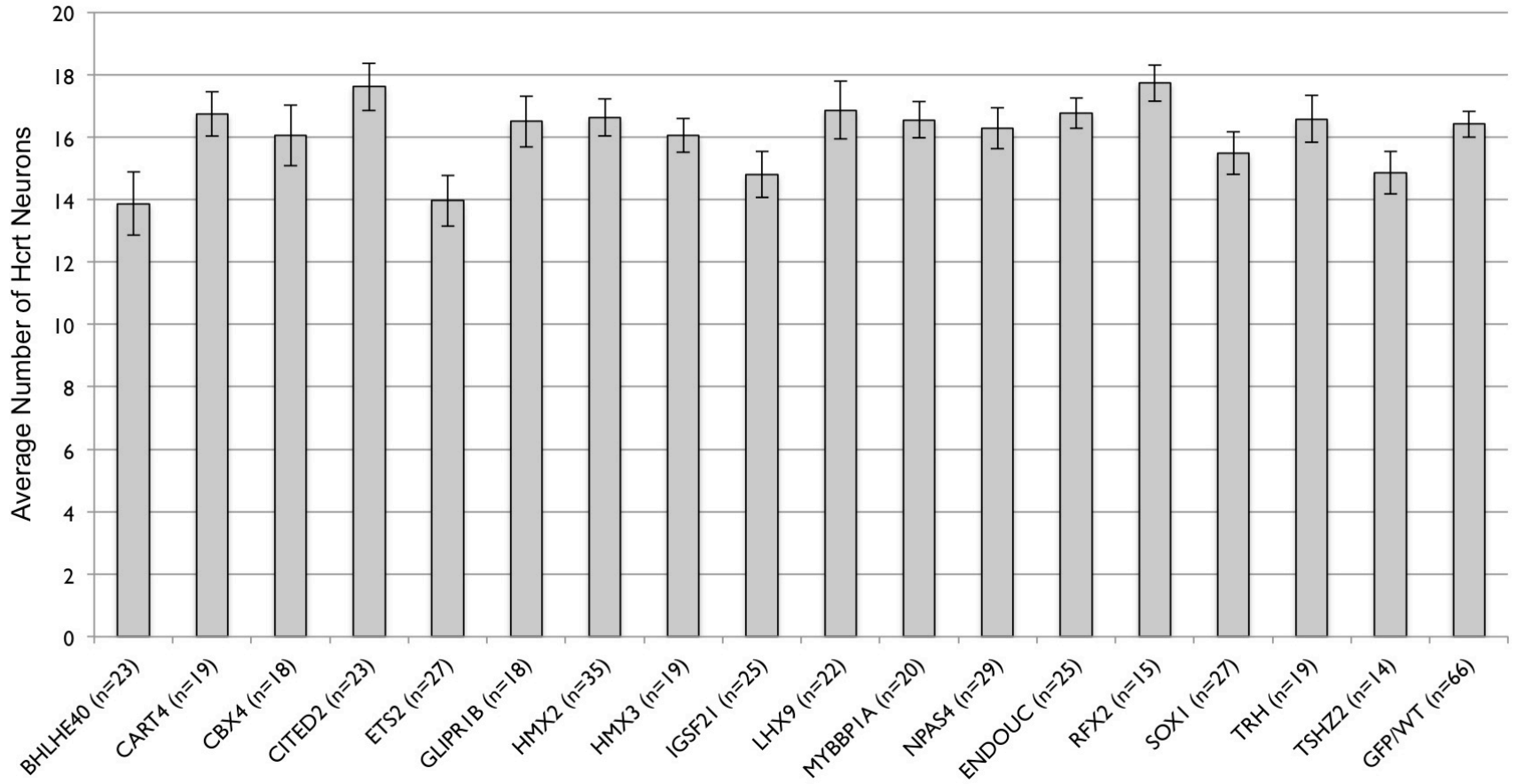
Average Number of Hcrt Neurons
0
2
4
6
8
10
12
14
16
18
20
BHLHE40 (n=23)
CART4 (n=19)
CBX4 (n=18)
CITED2 (n=23)
ETS2 (n=27)
GLIPR1B (n=18)
HMX2 (n=35)
HMX3 (n=19)
IGSF21 (n=25)
LHX9 (n=22)
MYBBP1A (n=20)
NPAS4 (n=29)
ENDOUC (n=25)
RFX2 (n=15)
SOX1 (n=27)
TRH (n=19)
TSHZ2 (n=14)
GFP/WT (n=66)

Figure S6

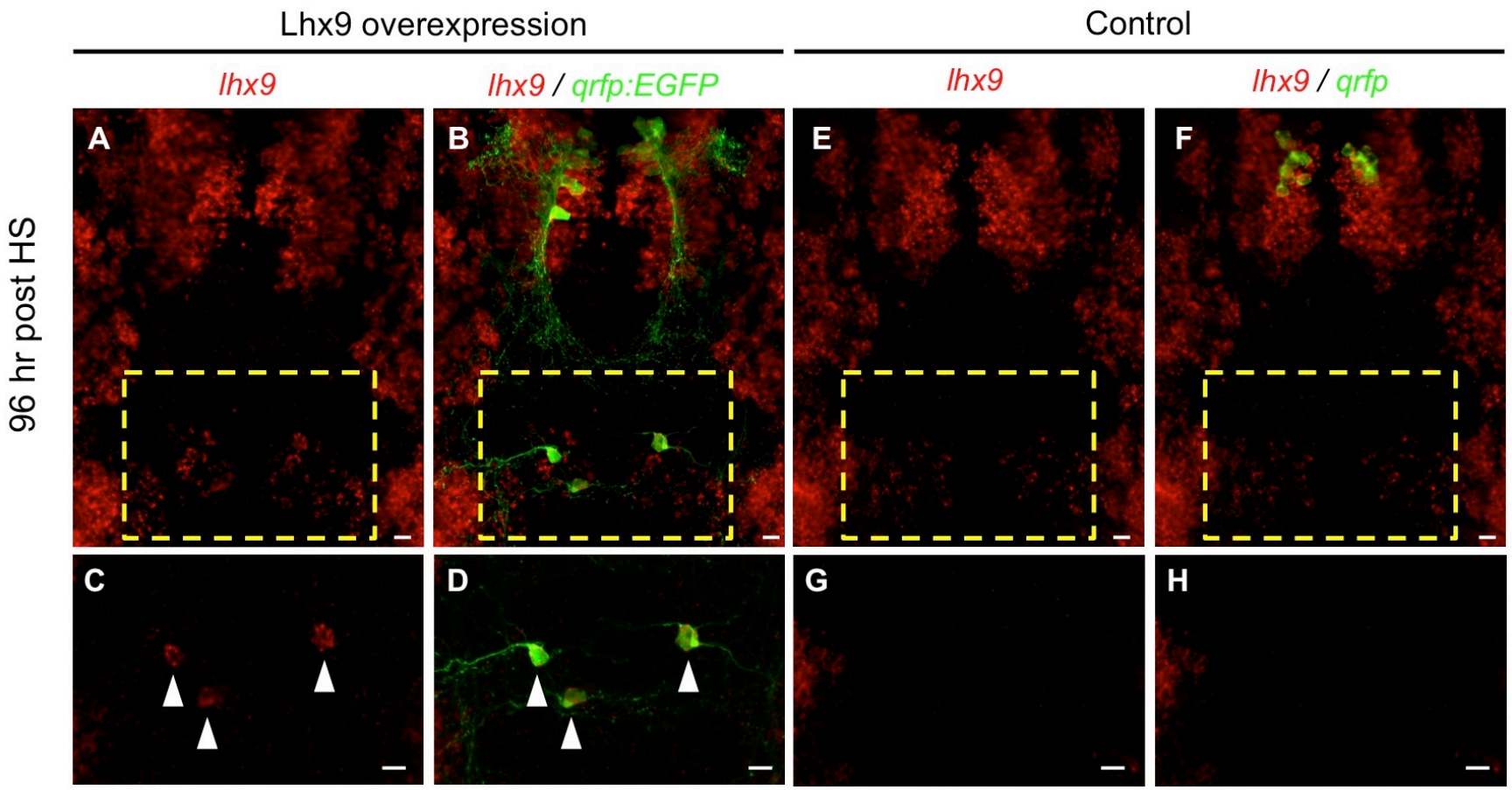
Lhx9 overexpression
Control
lhx9
lhx9 / qrfp:EGFP
lhx9
lhx9 / qrfp
96 hr post HS
A
B
C
D
E
F
G
H

Figure S7

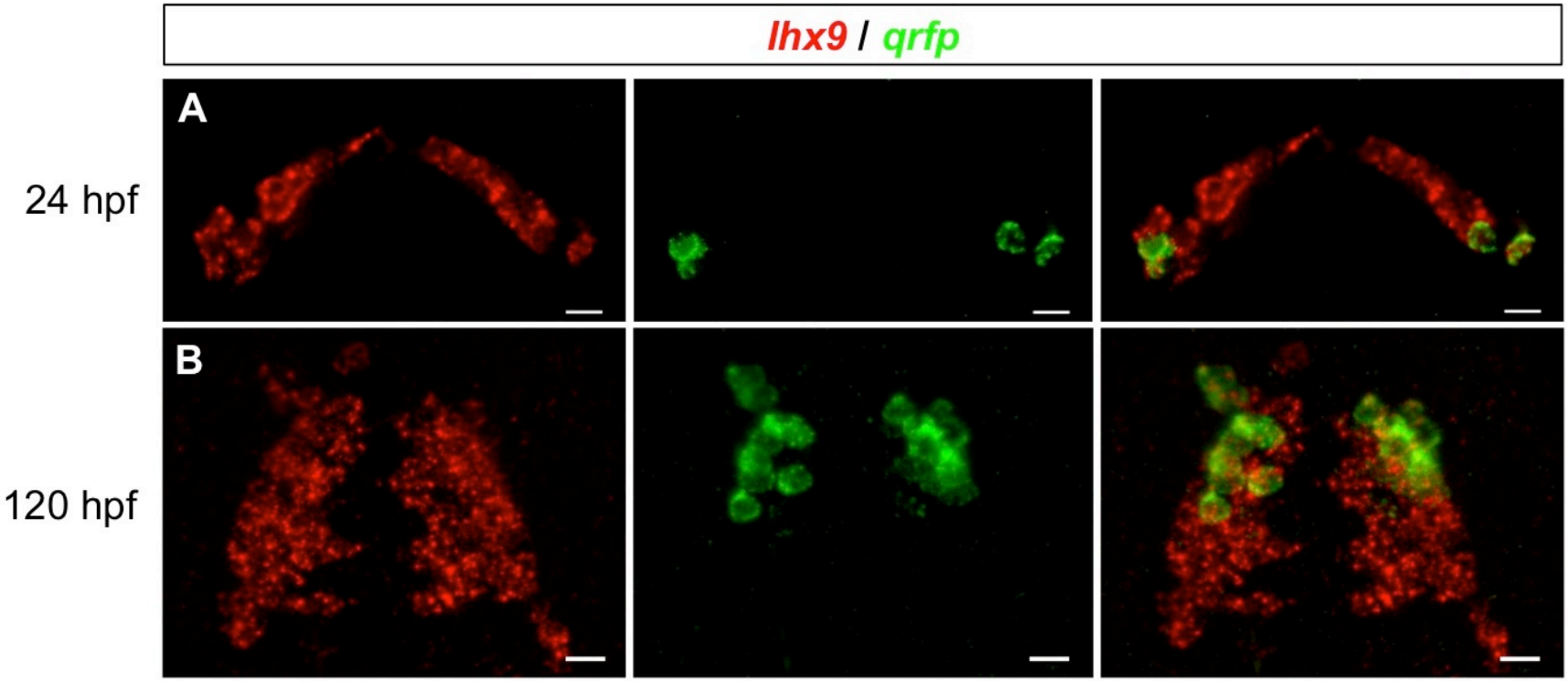

Figure S8

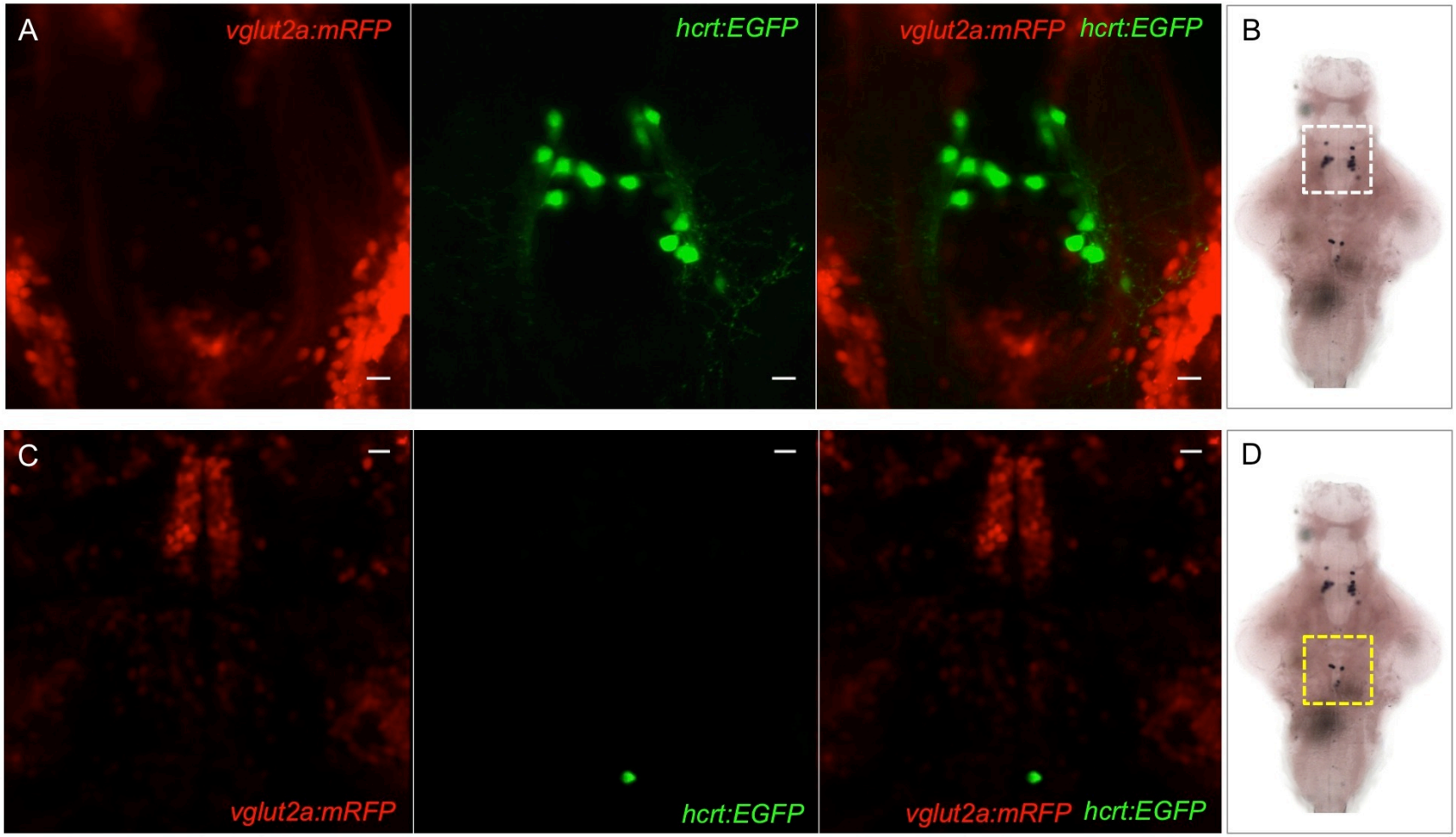
A
vglut2a:mRFP
hcrt:EGFP
vglut2a:mRFP hcrt:EGFP
B
C
vglut2a:mRFP
hcrt:EGFP
vglut2a:mRFP hcrt:EGFP
D

Figure S9

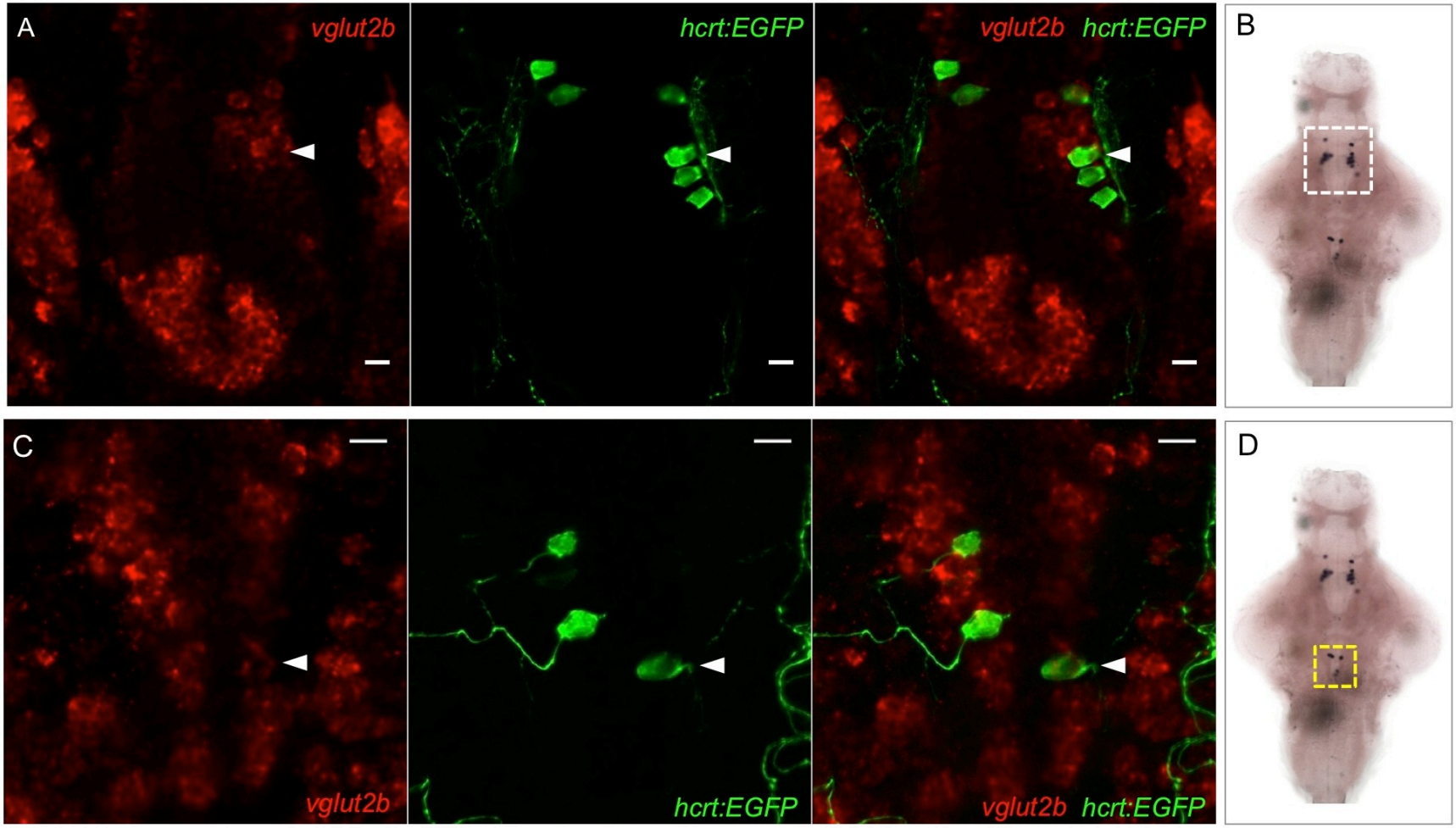
A
vglut2b
hcrt:EGFP
vglut2b hcrt:EGFP
B
C
vglut2b
hcrt:EGFP
vglut2b hcrt:EGFP
D

Figure S10

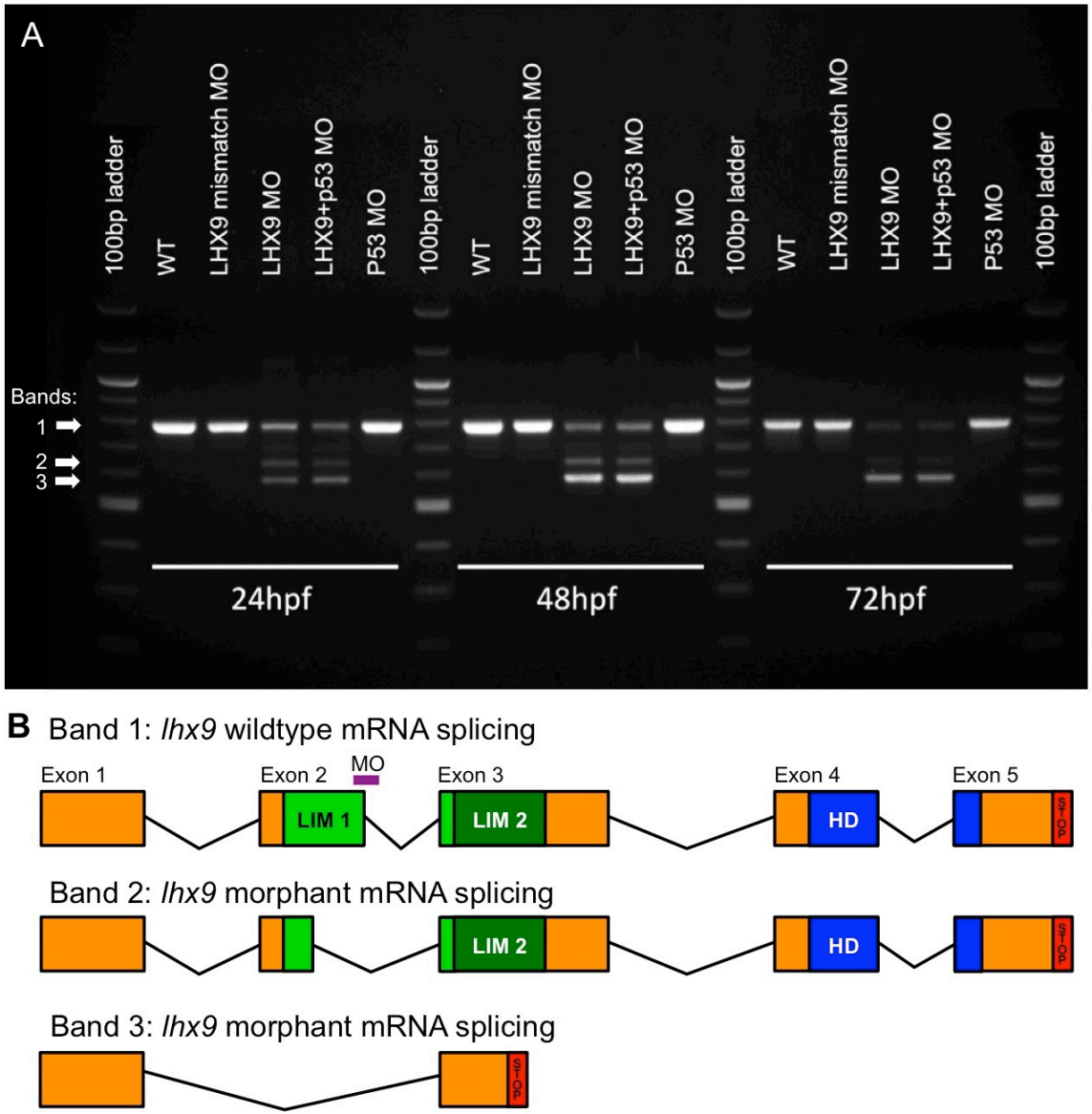
A
100bp ladder
WT
LHX9 mismatch MO
LHX9 MO
LHX9+p53 MO
P53 MO
Bands:
1
2
3
24hpf
48hpf
72hpf
B
Band 1: lhx9 wildtype mRNA splicing
Exon 1
Exon 2
MO
Exon 3
Exon 4
Exon 5
LIM 1
LIM 2
HD
Band 2: lhx9 morphant mRNA splicing
Band 3: lhx9 morphant mRNA splicing

Figure S11

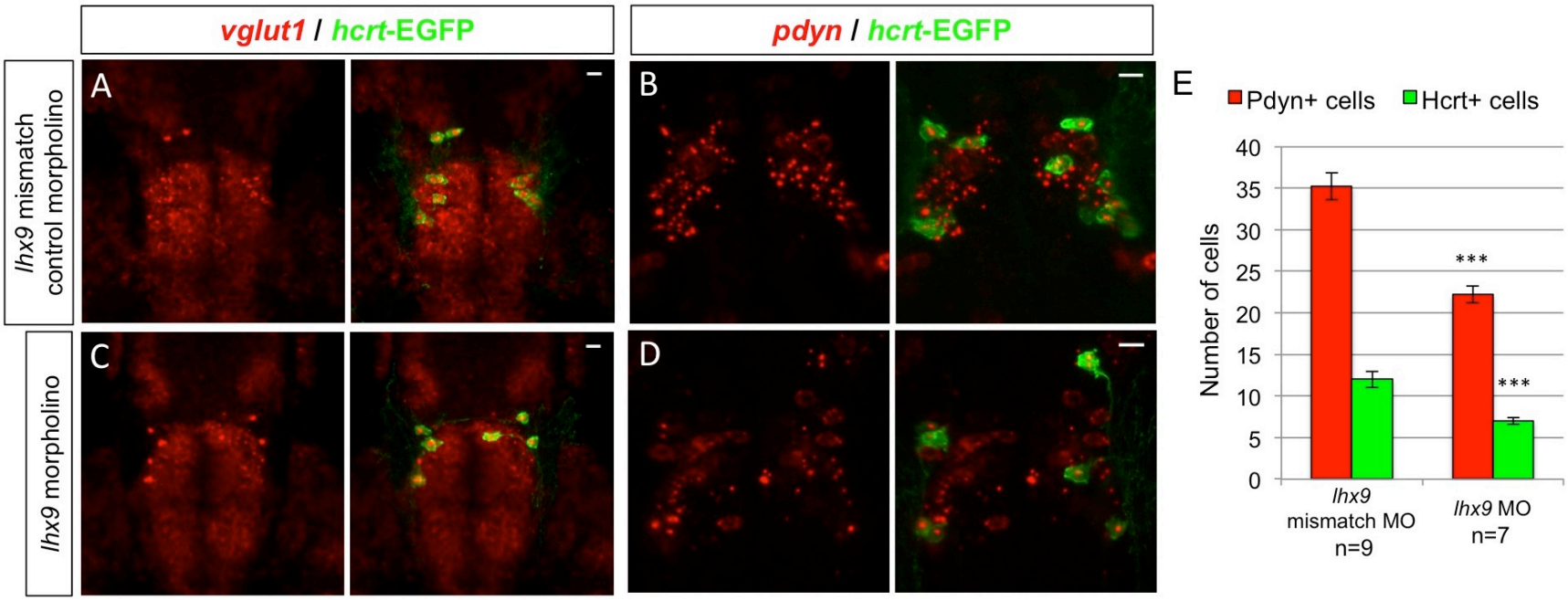
vglut1 / hcrt-EGFP
pdyn / hcrt-EGFP
lhx9 mismatch control morpholino
lhx9 morpholino
A
B
C
D
E
Pdyn+ cells
Hcrt+ cells
Number of cells
40
35
30
25
20
15
10
5
0
***
***
lhx9 mismatch MO n=9
lhx9 MO n=7

Figure S12

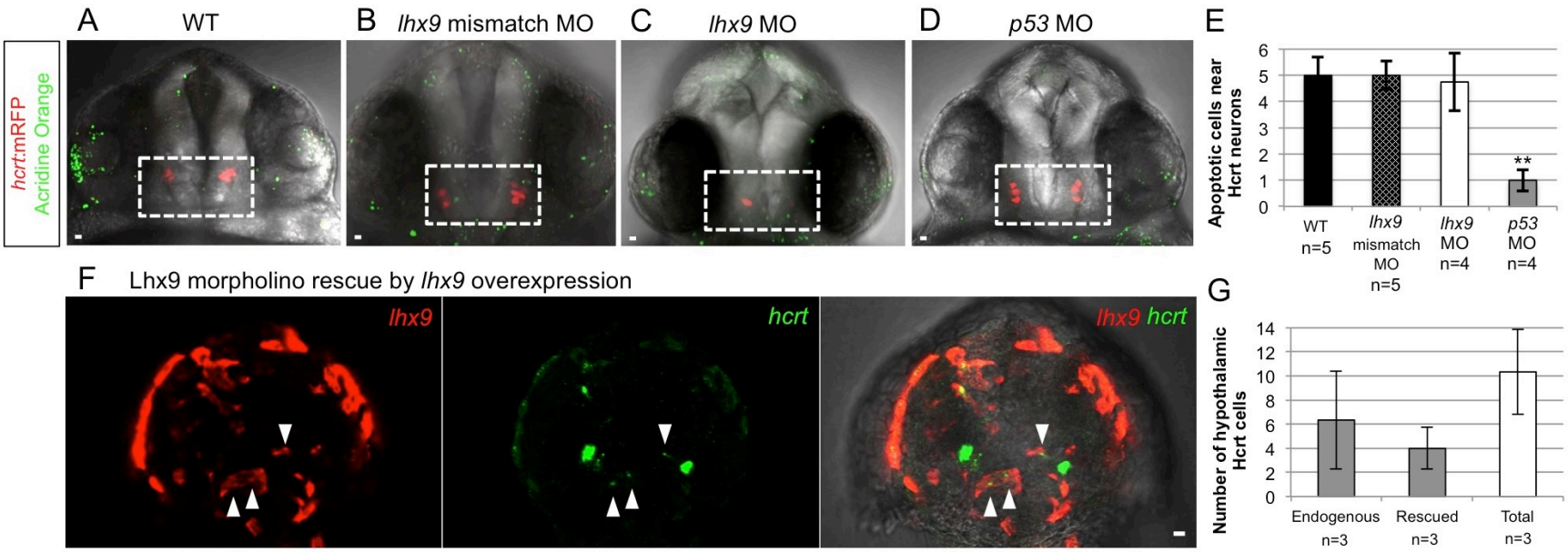
A WT
B lhx9 mismatch MO
C lhx9 MO
D p53 MO
hcrt:mRFP
Acridine Orange
E
Apoptotic cells near Hcrt neurons
WT n=5
lhx9 mismatch MO n=5
lhx9 MO n=4
p53 MO n=4
**
F Lhx9 morpholino rescue by lhx9 overexpression
lhx9
hcrt
lhx9 hcrt
G
Number of hypothalamic Hcrt cells
Endogenous n=3
Rescued n=3
Total n=3

Figure S13

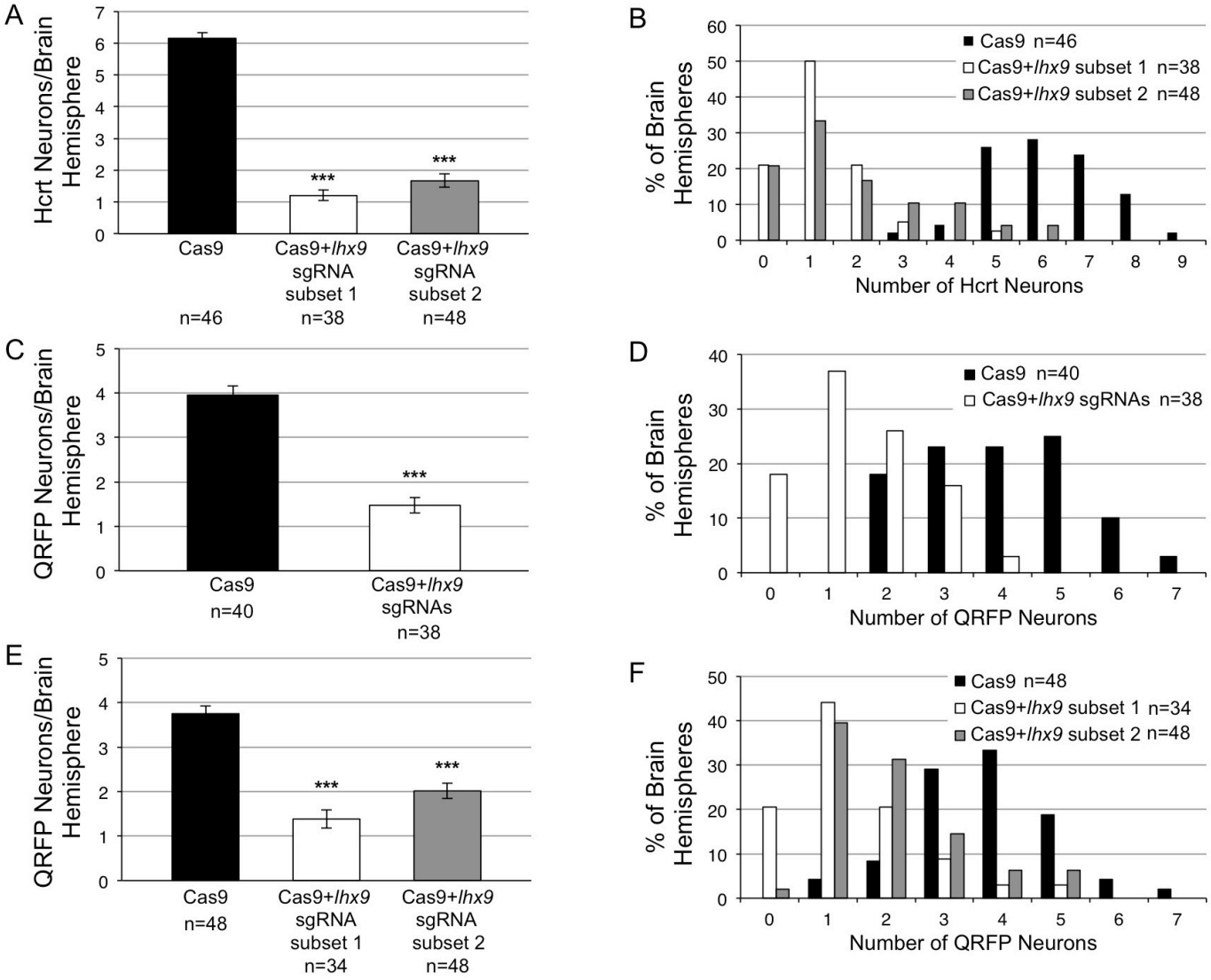
A
Hcrt Neurons/Brain Hemisphere
***
***
Cas9
n=46
Cas9+lhx9 sgRNA subset 1
n=38
Cas9+lhx9 sgRNA subset 2
n=48
B
% of Brain Hemispheres
Cas9 n=46
Cas9+lhx9 subset 1 n=38
Cas9+lhx9 subset 2 n=48
Number of Hcrt Neurons
C
QRFP Neurons/Brain Hemisphere
***
Cas9
n=40
Cas9+lhx9 sgRNAs
n=38
D
% of Brain Hemispheres
Cas9 n=40
Cas9+lhx9 sgRNAs n=38
Number of QRFP Neurons
E
QRFP Neurons/Brain Hemisphere
***
***
Cas9
n=48
Cas9+lhx9 sgRNA subset 1
n=34
Cas9+lhx9 sgRNA subset 2
n=48
F
% of Brain Hemispheres
Cas9 n=48
Cas9+lhx9 subset 1 n=34
Cas9+lhx9 subset 2 n=48
Number of QRFP Neurons

Figure S14

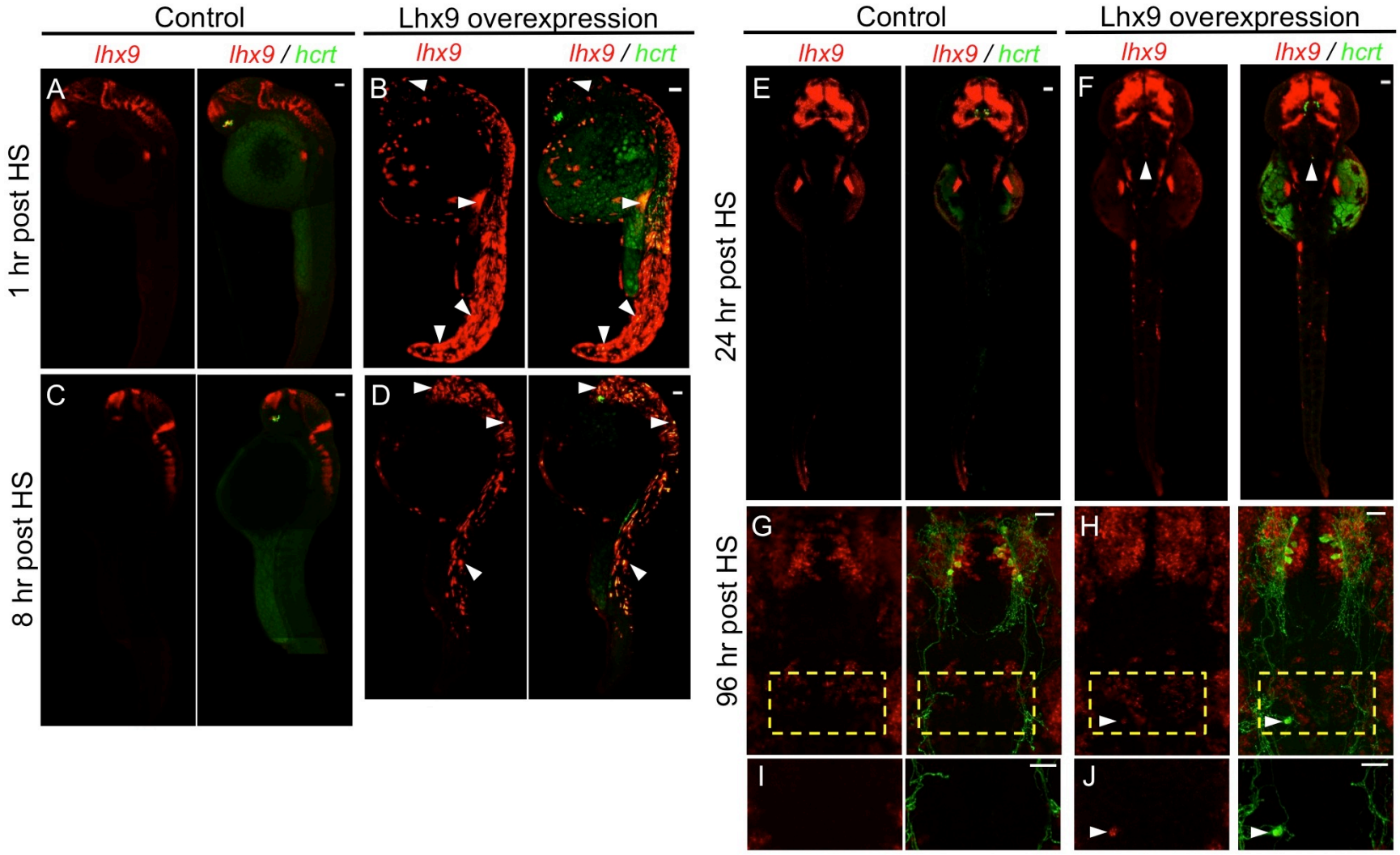
Control
Lhx9 overexpression
lhx9
lhx9 / hcrt
1 hr post HS
8 hr post HS
24 hr post HS
96 hr post HS
A
B
C
D
E
F
G
H
I
J

Figure S15

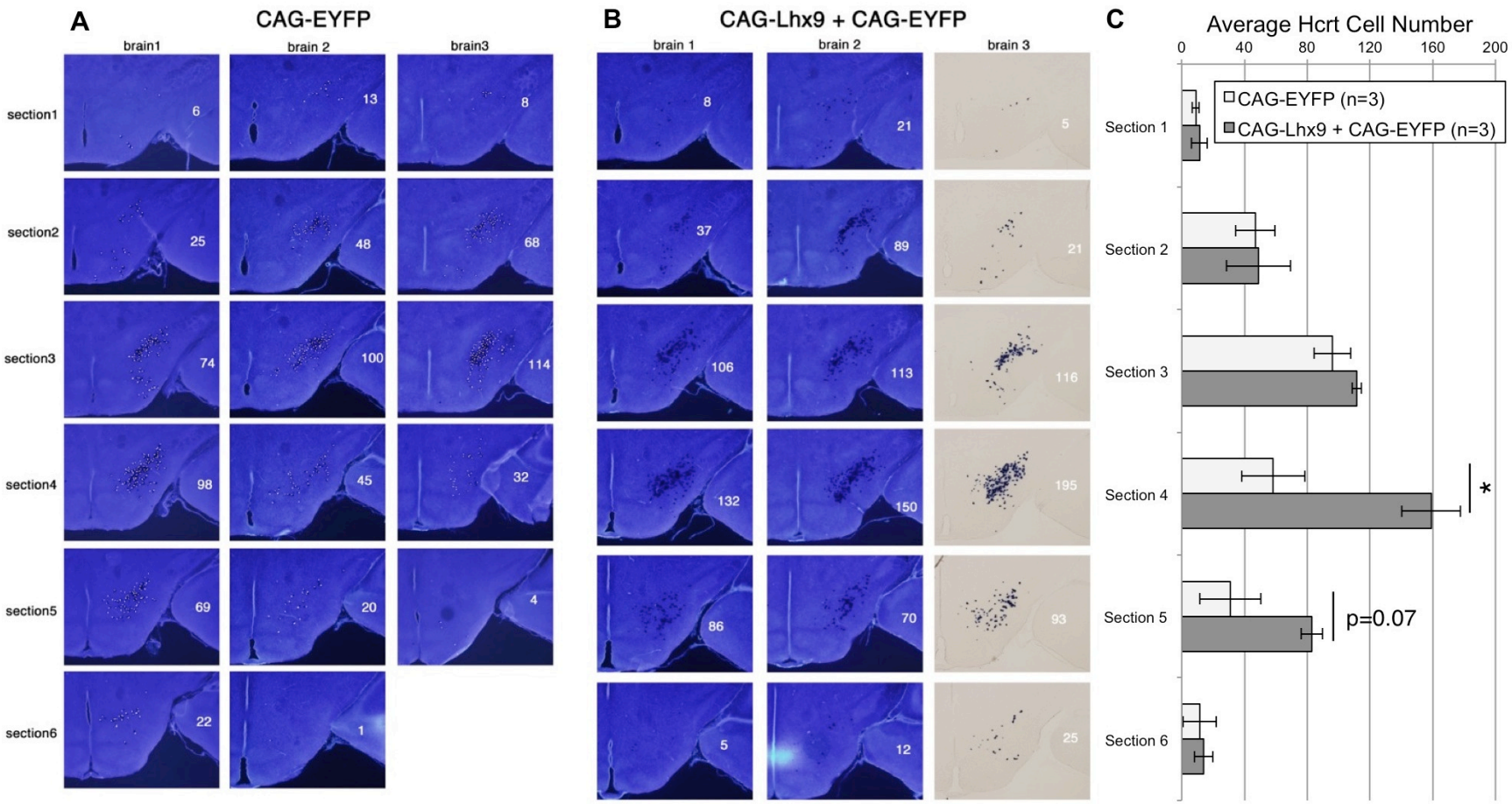
A
CAG-EYFP
brain1
brain 2
brain3
section1
section2
section3
section4
section5
section6
6
13
8
25
48
68
74
100
114
98
45
32
69
20
4
22
1
B
CAG-Lhx9 + CAG-EYFP
brain 1
brain 2
brain 3
8
21
5
37
89
21
106
113
116
132
150
195
86
70
93
5
12
25
C
Average Hcrt Cell Number
0
40
80
120
160
200
CAG-EYFP (n=3)
CAG-Lhx9 + CAG-EYFP (n=3)
Section 1
Section 2
Section 3
Section 4
Section 5
Section 6
*
p=0.07

Figure S16

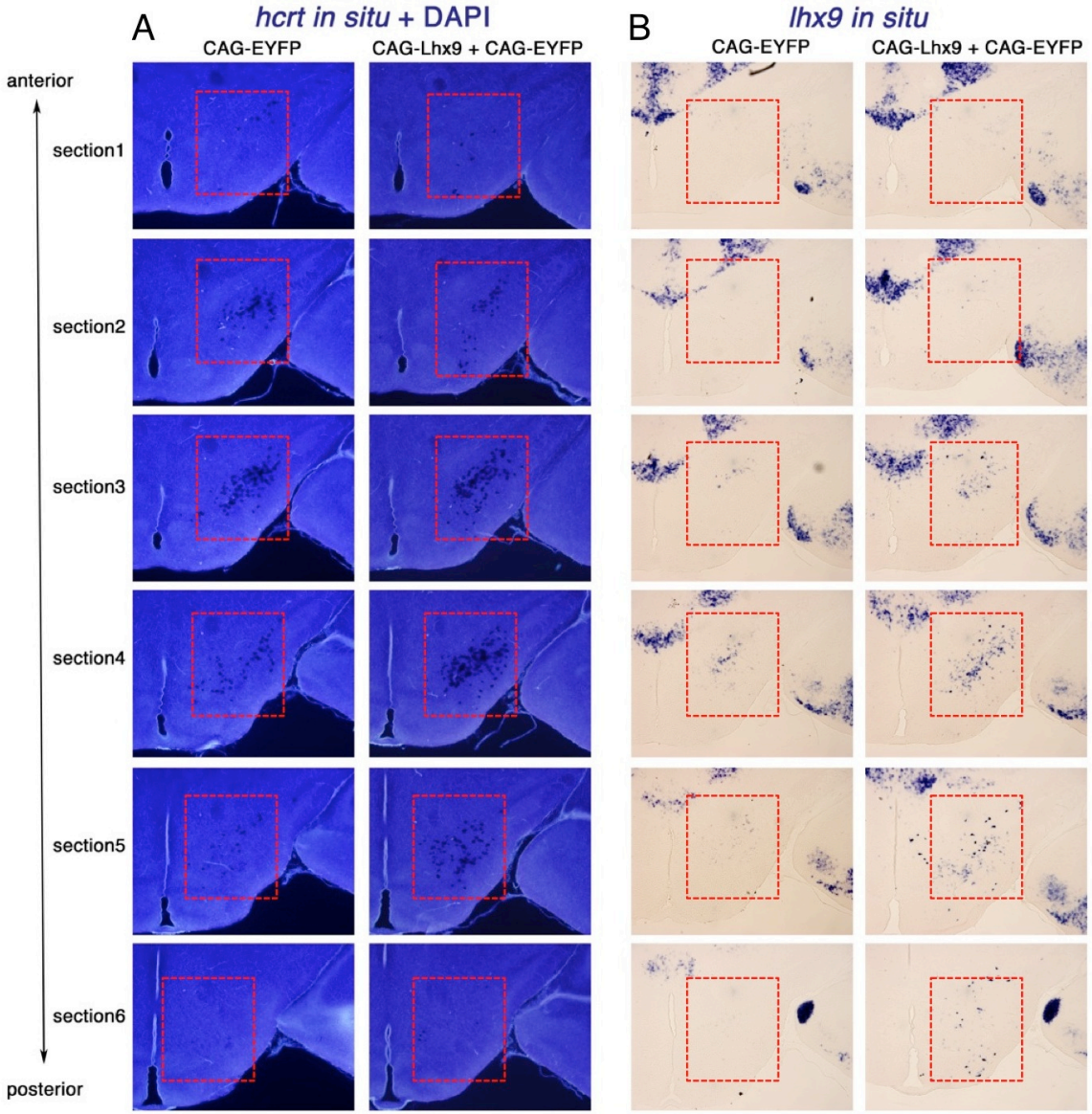
A
hcrt in situ + DAPI
CAG-EYFP
CAG-Lhx9 + CAG-EYFP
B
lhx9 in situ
CAG-EYFP
CAG-Lhx9 + CAG-EYFP
anterior
section1
section2
section3
section4
section5
section6
posterior

Figure S17

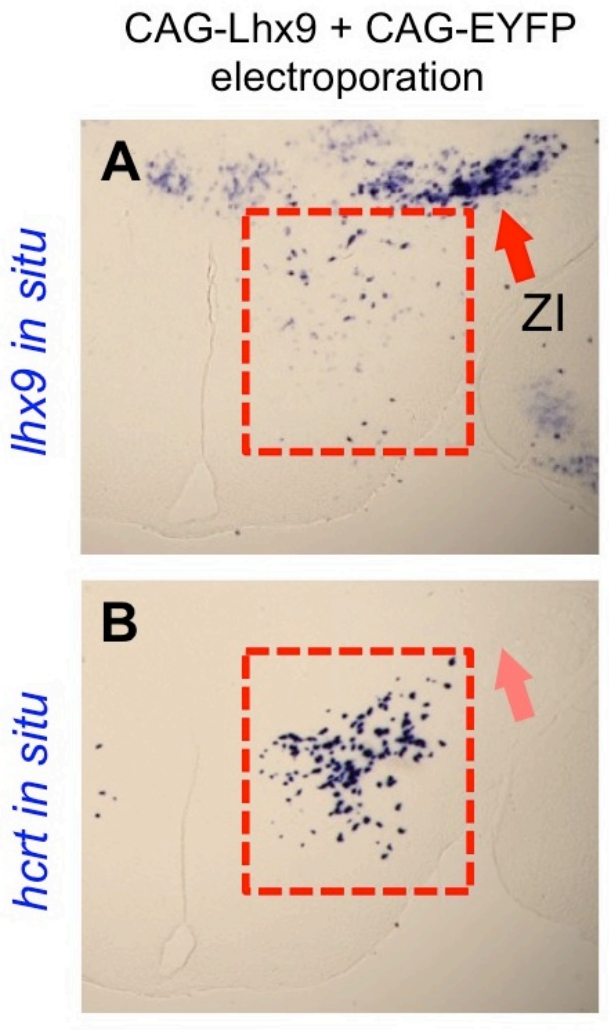
CAG-Lhx9 + CAG-EYFP
electroporation
A
Zl
lhx9 in situ
B
hcrt in situ

Movie 1. Colocalization of *hcrt-* and *lhx9*-expressing cells in the embryonic zebrafish hypothalamus. At 24 hpf, *lhx9* is expressed in the hypothalamus in bilateral clusters of 20-30 cells that overlap with *hcrt*-EGFP expressing cells. Note that all *hcrt*-EGFP cells also express *lhx9*. This movie shows the complete confocal image stack from which a single optical section is shown in Fig. 2F. Scale = 10 μm.

Movie 2. All hypothalamic Hcrt cells express *vglut1*. A 120 hpf *hcrt*-EGFP larva probed by fluorescent ISH for *vglut1* shows widespread expression of *vglut1* in the hypothalamus. After immunostaining with anti-GFP antibody, the sample was counterstained with DAPI to label cell nuclei. All Hcrt cells express *vglut1*, with particularly intense nuclear mRNA levels compared to adjacent neurons. This movie shows a confocal image stack advancing from the dorsal to the ventral hypothalamus. Scale = 10 μm.

Movie 3. All hypothalamic Hcrt cells express *pdyn*. A 120 hpf *hcrt*-EGFP larva probed by fluorescent ISH for *pdyn* shows that all Hcrt cells express *pdyn*, although *pdyn* is also expressed elsewhere in the hypothalamus. After immunostaining with anti-GFP antibody, the sample was counterstained with DAPI to label cell nuclei. Note that *pdyn* expression in Hcrt cells is observed as intense nuclear puncta that occupy a smaller area than the nucleus, potentially indicating a localized region of *pdyn* mRNA. This movie shows a confocal image stack advancing from the dorsal to the ventral hypothalamus. Scale = 10 μm.

Movie 4. Ectopic *lhx9*-expressing cells also express *hcrt* at one hour after heat shock. Embryos were injected with a HS-Lhx9 plasmid, fixed one hour after heat shock at 24 hpf, and analyzed using double fluorescent ISH with *hcrt*- and *lhx9*-specific probes. The intense green fluorescent cells are endogenous *hcrt*-expressing neurons. Endogenous *lhx9*-expressing neurons are not visible because this would require a higher laser power that would overexpose the fluorescence of ectopic *lhx9*-expressing cells. Anterior is to the left. The bright field (BF) overlay shows the position of the eye. This movie shows the complete confocal image stack from which a single optical section is shown in Fig. 7A.

Table S1

Click here to Download Table S1

Table S2

Click here to Download Table S2

Movie 1

Movie 2

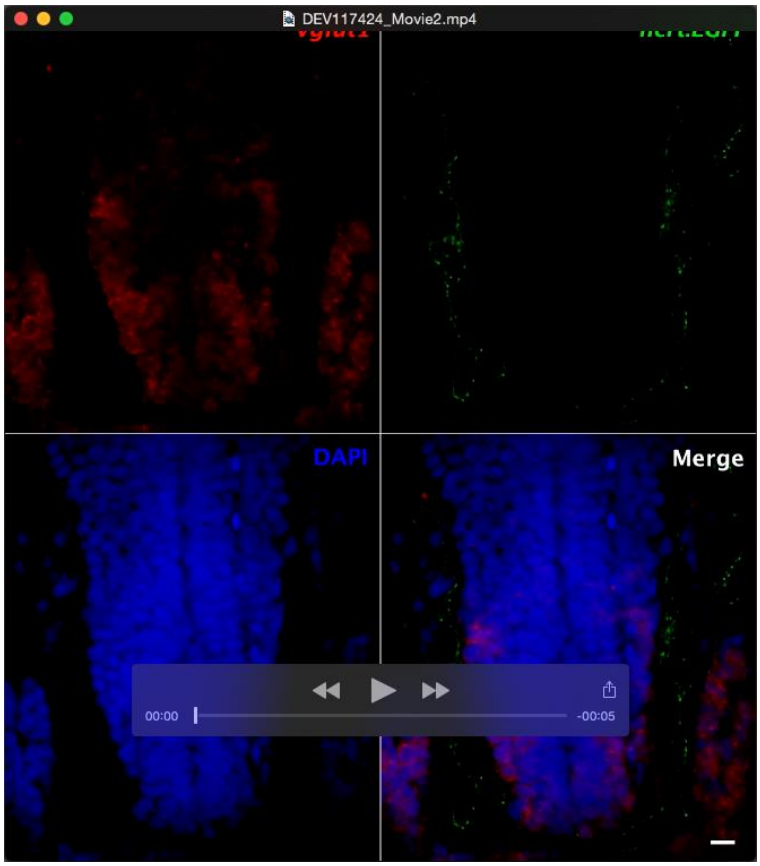

Movie 3

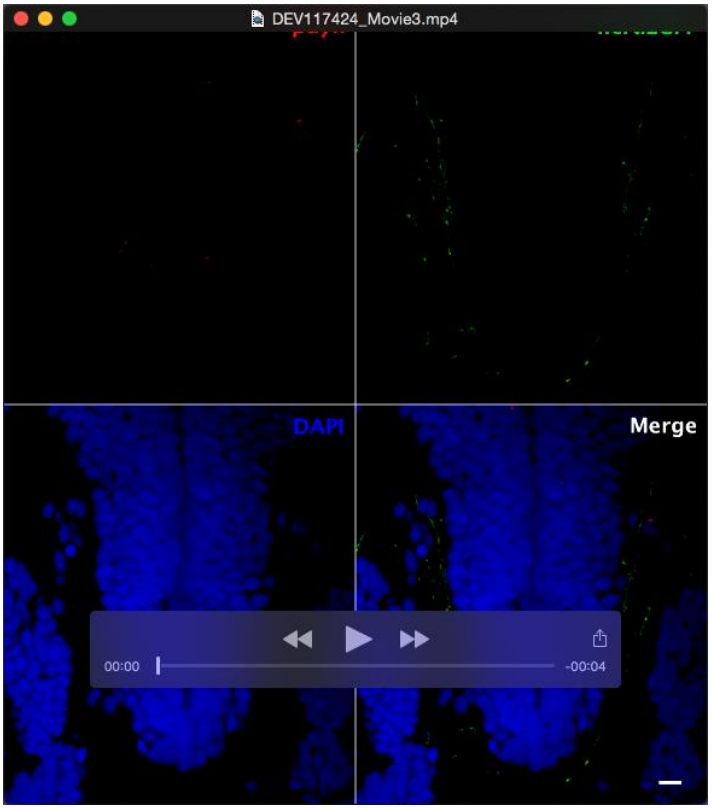

Movie 4